Board of Governors of the Federal Reserve System

International Finance Discussion Papers

ISSN 1073-2500 (Print)
ISSN 2767-4509 (Online)

Number 1434

March 2026

Volatile Rates, Fragile Growth: Global Financial Risk and Productivity Dynamics

Nils Gornemann, Eugenio Rojas, Felipe Saffie

Please cite this paper as:
Gornemann, Nils, Eugenio Rojas, Felipe Saffie (2026). "Volatile Rates, Fragile Growth: Global Financial Risk and Productivity Dynamics," International Finance Discussion Papers 1434. Washington: Board of Governors of the Federal Reserve System, https://doi.org/10.17016/IFDP.2026.1434.

Volatile Rates, Fragile Growth:

Global Financial Risk and Productivity Dynamics*

NILS GORNEMANN† EUGENIO ROJAS‡ FELIPE SAFFIE§

Federal Reserve Board *University of Florida* *University of Virginia & NBER*

March 6, 2026

Abstract

Does global financial risk affect long-run growth? Using a panel state-space model for emerging and advanced small open economies, we measure the effects of U.S. monetary policy uncertainty shocks. A one-standard-deviation shock lowers the level of the stochastic trend in emerging markets by at least 25 basis points after three years, with little effect in advanced economies. A small open economy model with growth through innovation and occasionally binding borrowing constraints explains this heterogeneity: higher interest-rate volatility depresses valuations, tightens collateral constraints, and slows innovation in equilibrium. A novel interaction between the occasionally binding constraint and stochastic volatility is key for our results.

Keywords: Endogenous Growth, Stochastic Interest Rate Volatility, Financial Frictions, Long-Term Productivity Trends, Global Financial Risk Cycle

JEL Classifications: F32, F41, G15, O16

*The views in this paper are solely the responsibility of the authors and should not be interpreted as reflecting the views of the Board of Governors of the Federal Reserve System or any other person associated with the Federal Reserve System. An earlier version of this paper was prepared for and first presented at the Philadelphia Federal Reserve–PIER–IER Conference in honor of Hal Cole. We thank Philippe Aghion, Andrés Blanco, Danilo Cascaldi-Garcia, V.V. Chari, Nicolas Coeurdacier, Hal Cole, Luca Dedola, Elias Dinopoulos, Jeremy Greenwood, Jonathan Heathcote, Peter Karadi, Narayana Kocherlakota, Julian Kozlowski, Alan Ledesma (discussant), Nels Lind, Enrique Mendoza, Pablo Ottonello, Diego Perez, Ricardo Reyes-Heroles, Juan Rubio-Ramírez, David Sappington, César Sosa-Padilla, Martín Uribe, Vivian Yue, and seminar participants at 2022 CEF, 2022 SEA, 2023 SED, 2024 CEMLA, 2024 EEA-ESEM, 2024 International Macro Finance Workshop at Jackson Hole, 2024 NASM, 2024 RIDGE December Forum, 2024 Spring Midwest Macro, 2025 Fall Midwest Macro, 2025 Gator Macro Workshop, 2025 LAEF-HKU, 2025 SED, UAI, and VII Santiago Macro Workshop; as well as at Binghamton University, the Chicago Fed, the ECB, Emory University, the IMF, LSE, Oxford, Sciences Po, the University of Nottingham, and the University of Oklahoma for their valuable comments. All remaining errors are our own.

†Board of Governors of the Federal Reserve System. Email: nilsgornemann@gmail.com.

‡Department of Economics, University of Florida. Email: erojasbarros@ufl.edu.

§Darden Business School, University of Virginia and NBER. Email: SaffieF@darden.virginia.edu.

1 Introduction

Emerging markets are vulnerable to shifts in global financial conditions. When perceived global economic risk increases –signaled by rising measures like the VIX or widening credit spreads– capital flows to emerging economies reverse sharply, exchange rates depreciate, and output contracts (Rey, 2015; Miranda-Agrippino and Rey, 2020). This sensitivity to global financial volatility is a defining feature of emerging market business cycles. These economies also exhibit substantially greater volatility in their trend growth than advanced economies (Aguiar and Gopinath, 2007). Are these two facts connected? Does global financial risk affect not only short run fluctuations but also the trajectory of long run productivity growth? This paper provides evidence that it does.

We estimate a panel state space model for two groups of small open economies, emerging markets and advanced economies, from 1993 to 2019. The model delivers estimates of the time varying growth rate of country specific trends in GDP, consumption, and investment, while decomposing each trend into two components, one driven by global financial uncertainty and one capturing all other sources of trend variation. Our baseline measure of global financial risk is an innovation to U.S. monetary policy uncertainty, identified as in Husted et al. (2020). We find that shocks to U.S. interest rate uncertainty generate persistent declines in the estimated stochastic trend of economic activity in emerging market economies, with no comparable effect in advanced economies. An increase in perceived uncertainty by one standard deviation lowers the level of the estimated trend in emerging markets by at least 25 basis points after three years with no resulting make up growth later in time. The result is robust across multiple measures of global financial uncertainty and remains when conditioning on U.S. macroeconomic and credit conditions. Advanced economies exhibit a significantly smaller response.

To explain these different responses, we develop a small open economy model with three key ingredients, endogenous productivity growth through innovation and firm entry, occasionally binding collateral constraints with firm value as collateral, and stochastic volatility in world interest rates. The mechanism operates through firms' investment into productivity enhancing innovations. Households own firms and can borrow internationally, but only up to a fraction of the present value of their firms' future profits. When interest rate volatility rises, the expected present value of these profits falls, both because households discount the future more heavily and because

large adverse interest rate shocks, which become more likely during high volatility periods, trigger sharp contractions when borrowing constraints bind. Lower firm values reduce innovation by incumbents and entry by new firms, depressing productivity growth.[1]

Crucially, the mechanism is asymmetric and relies on occasionally binding borrowing constraints. A large positive interest rate shock forces households to deleverage when the collateral constraint binds, sharply reducing consumption and raising the marginal utility of wealth. This amplifies the decline in firm valuations through a Fisherian deflation channel, falling asset values tighten borrowing conditions endogenously, creating a feedback loop between financial conditions and real activity. In contrast, when the constraint becomes slack, relaxing it further has little effect. As a result, an equally large negative interest rate shock provides limited stimulus. This asymmetry implies that, even holding fixed the average level of the world interest rate, higher volatility lowers collateral value and depresses innovation, with stronger effects in economies that enter the constrained region more often. In the quantitative exercise, we also allow the borrowing rate faced by the model economy to co-move with uncertainty, in line with previous work, to bring the model closer to the data. We show, however, that the asymmetry generated by occasionally binding constraints is key for reproducing the empirical patterns.

Calibrated to Mexico, the model replicates the differential response of emerging and advanced economies without targeting it. In the quantitative analysis, emerging and advanced economies share the same technology, preferences, and exposure to the world interest rate and volatility processes. They differ only in financial development parameters governing the pledgeability and the pricing of external borrowing. Three counterfactual experiments isolate the sources of the asymmetry. First, eliminating interest rate volatility reduces the coefficient of variation of trend growth in the emerging market calibration by about 30 percent while having negligible effects in the advanced economy calibration. Second, adjusting only financial development parameters, the fraction of firm value that can be collateralized and the sensitivity of borrowing costs to volatility, substantially narrows the gap in trend volatility between emerging and advanced economies. Third, differences in pledgeability account for roughly 60 percent of emerging markets' excess trend volatility, with the remaining share reflecting higher and more volatility sensitive risk pre-

[1] Our emphasis on firm values is consistent with the cross country evidence in Lakdawala et al. (2021). They show that rising U.S. monetary policy uncertainty predicts declining asset valuations abroad, especially in emerging market economies.

mia.

The model also matches observed patterns in the cross sectional distribution of growth rates. During periods of elevated U.S. interest rate volatility, the average trend growth falls in emerging markets and its dispersion across these countries rises sharply. Advanced economies exhibit stable, low dispersion throughout. When we simulate many economies facing common global financial shocks but idiosyncratic productivity draws, the model reproduces this pattern. Dispersion in trend growth spikes during high volatility periods in our emerging market model, as nonlinear amplification varies with countries' idiosyncratic states, but remains largely flat in the advanced economy version.

Our findings underscore the central role of financial development in shaping the long-run consequences of global financial risk. Volatility in global financial conditions is a largely unavoidable feature of the world economy. Our results show that the way this volatility interacts with domestic financial frictions determines whether it generates just temporary business cycle fluctuations or leaves permanent scars on productivity. Strengthening financial systems, through stronger legal enforcement, deeper financial markets, and more robust institutions, is, therefore, central to ensuring that periods of financial turbulence do not translate into persistent stagnation, especially for emerging markets.

Related Literature. Our contribution intersects three research areas.

First, volatility shocks in open economies. Classic open economy models (Mendoza, 1991; Neumeyer and Perri, 2005; Uribe and Yue, 2006) studied how fluctuations in world interest rate *levels* affect emerging markets, often through working capital constraints or exogenous correlation with productivity. More recent work examines second-moment shocks directly. Fernández-Villaverde et al. (2011) demonstrate that increasing interest rate volatility produces quantitatively noticeable effects on the level of activity through precautionary savings. Carrière-Swallow and Céspedes (2013) show uncertainty shocks generate larger output contractions in emerging than advanced economies. Bhattarai et al. (2020), Reyes-Heroles and Tenorio (2020), and Roch et al. (2025) extend this evidence to U.S. policy uncertainty and financial channels. Gruss and Mertens (2009) and Johri et al. (2022) emphasize volatility's role in Sudden Stops. Our empirical contribution shows second-moment shocks affect not just short-run output but also the *trend* component of growth. We measure this using multiple uncertainty proxies, including the VIX, macroeconomic uncer-

tainty (Jurado et al., 2015), and stochastic volatility in Treasury yields, and find robust evidence of persistent trend effects in emerging markets. Our theoretical contribution explains this through a mechanism linking volatility to firm valuation and innovation.

Second, the global financial cycle. Rey (2015) argues global risk drives capital flows and undermines monetary autonomy. Miranda-Agrippino and Rey (2020) show U.S. monetary policy shocks propagate worldwide, while Chari et al. (2022) document differential effects across financial institutions. Zhou (2024) and Gerding et al. (2014) highlight heterogeneity in investor types and capital market structure as source of heterogeneous effects. We isolate a distinct channel: internal financial frictions amplify volatility's impact on firm investment and productivity, so identical external shocks generate divergent outcomes.

Third, productivity trends and endogenous growth. Aguiar and Gopinath (2007) argue that a defining feature of emerging market cycles is large variation in *trend* growth—so that much of cyclical volatility reflects shocks to the trend rather than transitory deviations around a stable trend. Cerra and Saxena (2008) document that crisis events, which are more frequent in emerging market economies, are followed by highly persistent output losses rather than full recoveries, consistent with long-lived level effects. Garcia-Cicco et al. (2010) push the interpretation toward finance: when the model is disciplined with long samples, adding financial frictions and country-premium shocks markedly improves fit and assigns a smaller role to nonstationary productivity shocks.[2] Boz et al. (2011) provide a complementary information-based view, emphasizing learning about the trend-cycle decomposition. We bridge these views: *stationary* global financial shocks, especially changes in risk (second moments), can generate *persistent* movements in trend activity through financial amplification and endogenous productivity.

A broader lesson is that when productivity is endogenous, business-cycle shocks can spill into lower-frequency movements in activity; Comin and Gertler (2006) formalize this medium-run propagation through endogenous productivity dynamics, while Queralto (2020) offers an early application of their model to emerging market crisis. Our model builds on the dynamic version of Klette and Kortum (2004) developed by Ates and Saffie (2021) and embeds it in a collateral-constraint Sudden Stop framework in the spirit of Mendoza (2010). Closest in spirit, Benguria et al. (2022) study how Sudden Stops reshape firm/product dynamics (including export margins)

[2] Chang and Fernández (2013) find similar conclusions using quarterly data and Bayesian estimation.

and thereby generate persistent output and productivity losses, through a trade and reallocation mechanism distinct from our collateral-based innovation channel. Gornemann et al. (2025) develop the role of R&D-driven productivity dynamics for real exchange rates, emphasizing technology diffusion rather than our collateral-based innovation channel. Benigno et al. (2025) show that secular interest rate declines slow growth through misallocation. We add to this literature by focusing on the role of second-moment shocks in generating effects on the trend of activity in small open economies.[3]

Section 2 presents the empirical evidence. Section 3 develops the model. Section 4 presents the quantitative analysis. Section 5 concludes.

2 Empirical Evidence: Volatility and Persistent Output Losses

This section provides empirical evidence that U.S. interest rate uncertainty has permanent effects on economic performance across countries. Using a multivariate panel time-series framework, we estimate the impact of monetary policy uncertainty shocks on the *stochastic trend* components of GDP, consumption, and investment growth for both emerging and advanced economies. We find a clear pattern: uncertainty shocks systematically reduce the stochastic trend in emerging markets, while advanced economies are much less affected. This divergence is consistent with a volatility-driven propagation mechanism that is stronger in financially constrained environments.

2.1 Intuition for the approach

In principle, to capture long-lasting effects of uncertainty shocks on economic activity, it would be enough to regress GDP growth on many lags of the shocks and cumulate the coefficients, as in a local projection. We augment this approach with two restrictions that strengthen inference on low-frequency components.

First, consistent with both exogenous and endogenous growth models, we assume that GDP,

[3] In closed economies, Moran and Queralto (2018), Garga and Singh (2021), and Jordà et al. (2024) provide evidence that monetary policy shocks generate persistent output effects as firms adjust innovation.

consumption, and investment in country j share a common stochastic trend level,

$$A_{j,t} = \exp\left(\sum_{s=-\infty}^{t} \hat{a}_{j,s}\right),$$

where $\hat{a}_{j,s}$ denotes the time-varying trend growth rate.[4] As a result, the growth rates of log GDP ($\Delta y_{j,t}$), log consumption ($\Delta c_{j,t}$), and log investment ($\Delta i_{j,t}$) can be written as

$$\begin{pmatrix} \Delta y_{j,t} \\ \Delta c_{j,t} \\ \Delta i_{j,t} \end{pmatrix} = \begin{pmatrix} \alpha_j \\ \alpha_j \\ \alpha_j \end{pmatrix} + \begin{pmatrix} \Delta \tilde{y}_{j,t} \\ \Delta \tilde{c}_{j,t} \\ \Delta \tilde{i}_{j,t} \end{pmatrix} + \begin{pmatrix} 1 \\ 1 \\ 1 \end{pmatrix} \hat{a}_{j,t}.$$

Here α_j is the country-specific average growth rate. The terms $\Delta \tilde{y}_{j,t}$, $\Delta \tilde{c}_{j,t}$, and $\Delta \tilde{i}_{j,t}$ are stationary components capturing the cycle, while $\hat{a}_{j,t}$ captures permanent, common movement in the levels of the three series that we label the stochastic trend growth rate.

Second, we model the trend growth rate as the sum of (i) a residual persistent component and (ii) a distributed-lag effect of global uncertainty shocks:

$$\hat{a}_{j,t} = a_{j,t} + \sum_{s=0}^{n_\sigma} \eta_s \sigma_{t-s}^{MU},$$

where σ_t^{MU} denotes the monetary policy uncertainty shock at time t, and $a_{j,t}$ captures all other movements in trend growth. The $\{\eta_s\}$ are a direct estimate of the impulse response of the growth rate of the trend to a monetary policy uncertainty shock. The cumulative sum $\sum_{s=0}^{t} \eta_s$, therefore, measures the effect of an uncertainty increase t periods ago on the *level* of the stochastic trend in logs.

2.2 Data and proxies for interest rate uncertainty

We compile quarterly macroeconomic data from 1993Q1 to 2019Q4 for two country groups. The emerging market sample includes Argentina, Brazil, Chile, Mexico, the Philippines, South Africa, and Turkey. The advanced economy group consists of Australia, Canada, Denmark, New Zealand, Norway, and Sweden. We collect real GDP, consumption, and investment from the IMF's Interna-

[4] Many approaches impose related common-trend restrictions; see Bocola and Gornemann (2013) for a discussion.

tional Financial Statistics (IFS) database.[5] Due to missing observations, the panel is unbalanced. Our selection of countries follows Vicondoa (2019), which is fairly representative of the emerging market business cycle literature.

Our baseline proxy for interest rate uncertainty uses the text-based monetary policy uncertainty index in Husted et al. (2020). Following their approach, we construct an *innovation* to monetary policy uncertainty that is orthogonal to contemporaneous U.S. macroeconomic and financial conditions.[6] This innovation captures unexpected shifts in perceived U.S. interest rate risk conditional on those fundamentals.

In robustness checks, we replace this proxy with: (i) the VIX index; (ii) macro uncertainty from Jurado et al. (2015); and (iii) the stochastic volatility of real U.S. short rates following Fernández-Villaverde et al. (2011). These alternative proxies capture broader dimensions of global financial uncertainty beyond U.S. monetary policy alone.

2.3 Panel state-space model

We estimate a panel state-space model that separates low-frequency trend movements from higher-frequency cyclical dynamics. For each country j, the measurement equation is

$$\begin{pmatrix} \Delta y_{j,t} \\ \Delta c_{j,t} \\ \Delta i_{j,t} \end{pmatrix} = \begin{pmatrix} \alpha_j \\ \alpha_j \\ \alpha_j \end{pmatrix} + \Phi \left(\begin{pmatrix} \Delta y_{j,t-1} \\ \Delta c_{j,t-1} \\ \Delta i_{j,t-1} \end{pmatrix} - \begin{pmatrix} 1 \\ 1 \\ 1 \end{pmatrix} \hat{a}_{j,t-1} \right) + \begin{pmatrix} 1 \\ 1 \\ 1 \end{pmatrix} \hat{a}_{j,t} + B \cdot Z_t^{US} + \Sigma_j \epsilon_{j,t}^m,$$

where Φ governs the dynamics of the stationary cycle component, and Σ_j is a 3×3 diagonal matrix of country-specific measurement shock standard deviations.

The trend component is

$$\begin{aligned} \hat{a}_{j,t} &= a_{j,t} + \sum_{s=0}^{n_\sigma} \eta_s \sigma_{t-s}^{MU}, \\ a_{j,t} &= \rho_a a_{j,t-1} + \sigma_{j,a} \epsilon_{j,t}^a. \end{aligned}$$

In Z_t^{US} we control for current and lagged U.S. GDP growth and the excess bond premium

[5] We use gross fixed capital formation instead of capital formation as our investment measure to increase the number of periods covered in our sample.

[6] See appendix and Husted et al. (2020) for details.

from Gilchrist and Zakrajšek (2012). We also include n_σ growth rates of our uncertainty series to capture transitory co-movement at business-cycle frequencies. This specification imposes a separation between (i) effects of uncertainty on the stochastic trend (through η_s) and (ii) higher-frequency effects absorbed by Z_t^{US}.

Shocks $(\epsilon_{j,t}^m, \epsilon_{j,t}^a)$ are drawn from a joint normal distribution. The deterministic trend α_j and shock variances are country specific, while the remaining parameters are common across countries in each panel, a standard restriction in panel models for small open economies (e.g. Uribe and Yue (2006), Akıncı (2013), Vicondoa (2019)). As the effects of uncertainty shocks are often found to build over time, we set $n_\sigma = 12$ quarters to capture effects up to three years.[7]

Estimation proceeds by maximum likelihood using the Kalman filter. Standard errors are obtained via monte carlo simulations, re-estimating the entire state-space model in each replication, so confidence intervals for impulse responses account for uncertainty about both the filtered trend and its response to uncertainty among other things. The uncertainty shock σ_t^{MU} is common across all countries in a given panel: each emerging and advanced economy is exposed to the same sequence of global monetary policy uncertainty innovations. Differences in responses therefore reflect differences in internal propagation, not differences in the shock processes themselves.[8]

2.4 Results

Figure 1 shows the estimated cumulative impulse response of the stochastic trend to a one-standard-deviation monetary policy uncertainty shock, $\sum_{s=0}^{t} \eta_s$. Advanced economies exhibit small and typically statistically weak responses. Emerging markets instead experience a sharp and persistent decline in the stochastic trend.

Because the unrestricted η_s can be noisy at longer horizons, we also report results imposing a flexible functional form on the lag profile of η_s. This restriction is a regularization device: it is not required for the qualitative result, emerging market economies respond a lot more than advanced economies, but it produces smoother impulse responses and reduces sensitivity to high-frequency variation being attributed to the trend component. Following Barnichon and Matthes (2018), we set $\eta_s = a \exp\left(-\frac{s-b}{c}\right)$ and estimate a, b, c jointly with the other parameters. The restricted esti-

[7] We verified that our results are robust to different lengths of this window.

[8] When constructing standard errors we incorporate that all countries face the same sequence of U.S. observations.

mates are plotted as solid lines in Figure 1 and are used for the baseline confidence bands.

Figure 1: Trend Response to Monetary Policy Uncertainty Shock

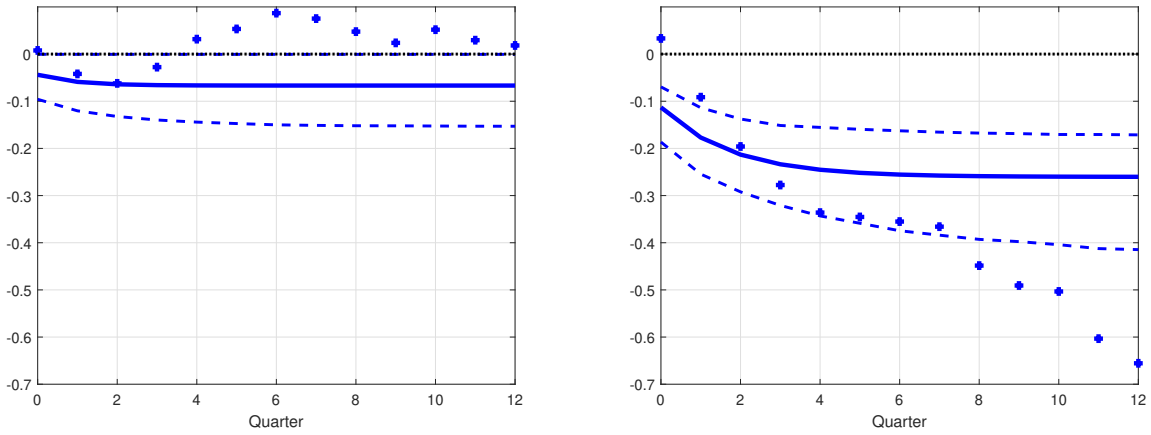

(a) Advanced Economies (b) Emerging Market Economies

Notes: The figure reports the cumulative effect of a monetary policy uncertainty shock on the trend after s quarters ($\sum_{t=0}^{s} \eta_t$). The solid line shows the point estimate when the functional form for η_s is imposed; bands represent one-standard-deviation confidence intervals. Dots denote the point estimate when no functional form is imposed.

In terms of magnitude, at a 12-quarter horizon the estimated decline in EMEs is between about 25 and 65 basis points, depending on whether we impose a parametric restriction on the lag profile of η_s (about 25 basis points under the restricted specification; about 65 basis points under the unrestricted estimates).[9]

Figure 2 confirms that the findings are robust across alternative uncertainty proxies. We replace the monetary policy uncertainty innovation with: (1) the VIX index; (2) macro uncertainty from Jurado et al. (2015); and (3) the stochastic volatility of real U.S. short rates following Fernández-Villaverde et al. (2011).[10] We focus on the parametric case in the figures. While magnitudes vary across proxies, the ordering is stable: responses are notably larger for emerging markets than for advanced economies. In addition, for proxies more tightly connected to interest rate uncertainty, the long-horizon effect on advanced economies is fairly close to zero.[11]

[9] It is worth keeping in mind that $\sum_{s=0}^{t} \eta_s$ is the percent deviation in the *level* of the estimated stochastic trend relative to baseline at horizon t after an uncertainty shock.

[10] The volatility measure employed in Figure 2 is the stochastic volatility of the U.S. real interest rate (Fernández-Villaverde et al., 2011). Appendix A.1 describes the estimation procedure and results.

[11] Figure 12 in the appendix provides the confidence intervals for each case.

Figure 2: Trend Response to Uncertainty Shocks, Robustness: Shock Proxies

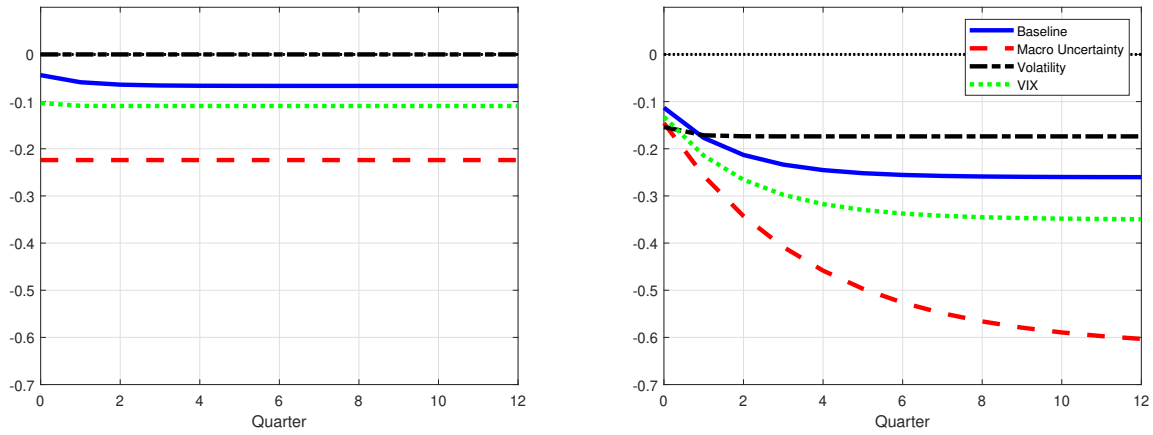

(a) Advanced Economies (b) Emerging Economies

Notes: This figure plots the cumulative response of the estimated stochastic trend to a one-standard-deviation global uncertainty shock for advanced economies (panel a) and emerging economies (panel b). The "Baseline" line reproduces the response to the monetary policy uncertainty innovation used in Figure 1. The other lines report responses when the uncertainty shock is proxied by (i) the VIX index, (ii) macroeconomic uncertainty from Jurado et al. (2015), and (iii) the stochastic volatility of the U.S. real short rate following Fernández-Villaverde et al. (2011). All responses are estimated under the parametric restriction on η_s and include the same set of U.S. controls as in the baseline specification.

2.5 Empirical estimates of trend growth

We now examine the cross-sectional dynamics of estimated trend growth across countries. Figure 3 displays the cross-sectional average and standard deviation of country-specific trend growth, demeaned within country, for emerging market and advanced economies over quarters with full data coverage. For each quarter, we subtract each country's sample mean of the filtered trend growth rate and compute, within each group, the cross-sectional average and dispersion.[12]

Two patterns stand out. First, average trend growth among advanced economies is relatively stable. Emerging markets, by contrast, exhibit much larger fluctuations in trend growth, especially during and after the Global Financial Crisis. Second, Emerging Market economies show persistently greater cross-sectional dispersion, with a sharp spike during 2008–2009 that remains elevated for years.

[12]Figure 3 uses quarterly data from 2000Q3 onward, which is the first date at which both the advanced and emerging economy samples are simultaneously balanced.

Figure 3: Cross-Sectional Moments of the Stochastic Trend Growth Rate

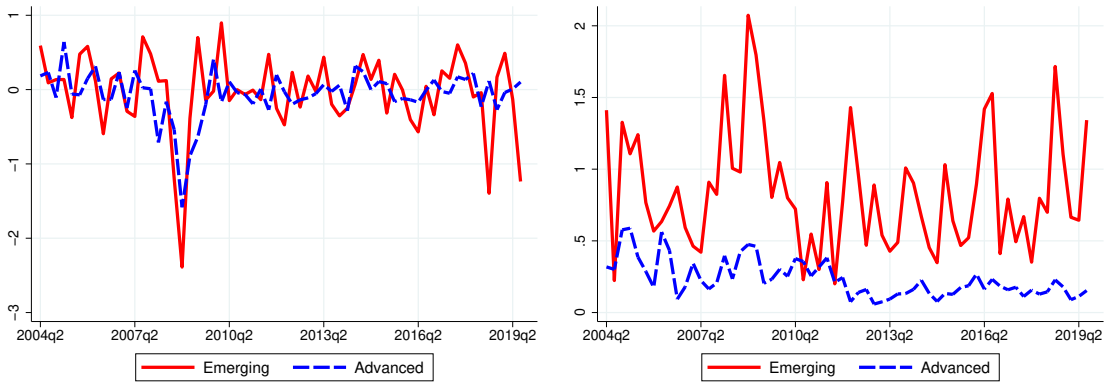

(a) Cross-Sectional Average (b) Cross-Sectional Standard Deviation

Notes: This figure shows cross-sectional moments of the estimated country-specific stochastic trend growth rates for advanced economies and emerging market economies. In each quarter, we subtract each country's average trend growth (over the sample) from its filtered trend growth rate and then compute, within each group, the cross-sectional average (panel a) and cross-sectional standard deviation (panel b). The underlying trends are obtained from the panel state-space model described in Section 2, using common global uncertainty shocks and U.S. controls for all countries.

These patterns are consistent with the model mechanism developed in Section 4: common volatility shocks generate disproportionately heterogeneous outcomes in financially constrained economies. In Section 4 we show that the calibrated model reproduces both the lower average trend growth and the higher cross-sectional dispersion of emerging markets in periods of elevated U.S. interest rate volatility.

3 A Small Open Economy with Volatility-Driven Trend Dynamics

3.1 Model Overview

We develop a small open economy model in which volatility in global interest rates, beyond changes in their level, drives persistent fluctuations in long-run productivity growth. The mechanism operates through an occasionally binding collateral constraint on borrowing and endogenous firm dynamics. A representative household owns a continuum of intermediate good producers and can borrow externally by pledging shares in firms as collateral. The borrowing terms depend not only on the level of the global interest rate but also on its volatility, introducing a channel through which financial conditions affect growth.

The engine of long-run growth is creative destruction among intermediate good producers.

Firms expand, contract, or exit through innovation and competition following the framework of Klette and Kortum (2004). These firms sell differentiated intermediate goods to a final good producer, which aggregates inputs into a single tradable final good under an aggregate efficiency (TFP) shock.

Our model extends traditional endogenous Sudden Stop frameworks in three key ways. First, collateral is based on the value of firms' future profits, directly tying innovation dynamics to borrowing capacity. Second, endogenous technical change determines the evolution of firm value through productivity-enhancing investment and firm entry. Third, both the level (first moment) and volatility (second moment) of international interest rates influence firm dynamics, collateral values, and innovation incentives. Together, these elements generate an endogenous link from second-moment financial shocks to persistent trend growth outcomes. The key equilibrium objects are the household's stochastic discount factor and the economy-wide creative destruction rate, which together determine the evolution of aggregate productivity and thus the trend.

3.2 Households

The representative household chooses consumption C and non-state-contingent bond holdings B^H each period. Labor supply $\bar{L}$ is inelastic and remunerated at wage w. In addition to labor income, the household receives lump-sum transfers T from incumbent firms, which it owns.

The household solves:

$$\max_{C(s^t),\, B^H(s^t)} \sum_{t=0}^{\infty} \beta^t \mathbb{E}\left[\frac{1}{1-\gamma}\left[C(s^t)\right]^{1-\gamma} \middle| s_0\right] \tag{1}$$

subject to:

$$C(s^t) + \hat{q}(s^t) B^H(s^t) \leq w(s^t)\bar{L} + B^H(s^{t-1}) + T(s^t), \tag{2}$$

$$\hat{q}(s^t) B^H(s^t) \geq -\phi V(s^t). \tag{3}$$

Here $\hat{q}(s^t)$ denotes the price of debt, defined as the reciprocal of the gross interest rate faced by households, $\hat{R}(s^t) \equiv 1/\hat{q}(s^t)$. The household faces a collateral constraint: it cannot borrow more than a fraction ϕ of the total value of incumbent firms $V(s^t)$, which it owns.

This structure departs from traditional models of endogenous financial crises (Bianchi and

Mendoza, 2018), where collateral is typically tied to tradable income or physical assets. Instead, consistent with private equity and venture capital practices, the household uses the value of future firm cash flows as collateral. This formulation aligns with recent empirical evidence on earnings-based borrowing constraints (Lian and Ma, 2021; Drechsel, 2023), and mirrors credit assessment practices in traditional banking, where project valuations and expected cash flows discipline credit limits.

3.3 Financial Intermediaries

Households borrow from competitive, risk-averse international financial intermediaries. Intermediaries face a stochastic gross funding cost R and lend to households at price $\hat{q}$. The gross funding cost evolves according to an AR(1) process with stochastic volatility:

$$R(s^t) - \bar{R} = \rho_R \left(R(s^{t-1}) - \bar{R} \right) + \sigma_R(s^t)\, \omega(s^t), \quad \omega(s^t) \sim N(0,1), \tag{4}$$

$$\log\big(\sigma_R(s^t)\big) = (1-\rho_\sigma)\mu_\sigma + \rho_\sigma \log\big(\sigma_R(s^{t-1})\big) + \eta_\sigma \nu(s^t), \quad \nu(s^t) \sim N(0,1), \tag{5}$$

where $\bar{R}$ denotes the average funding cost, ρ_R and ρ_σ govern the persistence of the funding cost and its volatility, and $\sigma_R(s^t)$ denotes the conditional standard deviation of the funding shock.

Intermediaries price household debt by solving:

$$\max_{b(s^t)} \mathbb{E}\Big[\hat{m}(s^{t+1})\, b(s^t) \mid s^t\Big] - \hat{q}(s^t)\, b(s^t), \tag{6}$$

where $\hat{m}(s^{t+1})$ is the intermediaries' stochastic discount factor. To capture their risk sensitivity to volatility, we assume:

$$\hat{m}(s^{t+1}) = \frac{1}{R(s^{t+1}) + \iota_0 + \iota_1 \left(\sigma_R(s^{t+1}) - \bar{\sigma}_R\right)},$$

where ι_0 captures a baseline spread and $\iota_1 > 0$ captures the degree to which spreads widen in response to higher interest rate volatility.

This reduced-form specification is consistent with models of intermediary frictions under stochastic volatility, such as Gertler and Karadi (2011) and Gertler and Kiyotaki (2015). Appendix B presents a formal model with these features, showing how increased volatility in funding costs raises loan spreads. Alternatively, this structure is consistent with ambiguity aversion (see Bianchi

et al. (2018a)), and similar reduced-form pricing structures have been employed in Arellano and Ramanarayanan (2012), Bianchi et al. (2018b), Johri et al. (2022), and Hegarty et al. (2023).

The solution to (6) yields the bond pricing function:

$$\hat{q}(s^t) = \mathbb{E}\left[\frac{1}{R(s^{t+1}) + \iota_0 + \iota_1 \left(\sigma_R(s^{t+1}) - \bar{\sigma}_R\right)} \,\middle|\, s^t \right]. \tag{7}$$

Expected spreads therefore rise with volatility, even when the conditional mean of R is unchanged. Foreign intermediaries' pricing rule determines the wedge between the exogenous world funding cost and the domestic borrowing rate, while households discount cash flows using their own stochastic discount factor. The two objects capture different sources of risk and are linked through the bond price $\hat{q}(s^t)$.

3.4 Final Good Producer

The final good producer aggregates a mass Λ of differentiated intermediate goods into a single homogeneous final output using a Cobb–Douglas-like technology:

$$\ln Y(s^t) = z(s^t) + \frac{1}{\Lambda} \int_0^{\Lambda} \ln y_i(s^t)\, di, \tag{8}$$

where $Y(s^t)$ denotes the final good, $y_i(s^t)$ is the demand for intermediate variety i, and $z(s^t)$ is an aggregate efficiency (TFP) shock.

The aggregate efficiency shock follows an AR(1) process:

$$\ln z(s^t) = \rho_z \ln z(s^{t-1}) + \epsilon_t, \quad \epsilon_t \sim N(0, \eta_z^2),$$

where ρ_z governs persistence and η_z the volatility of aggregate productivity innovations. The final good is the only tradable output in the economy and serves as the numeraire for international borrowing and lending.

3.5 Intermediate Good Producers

A continuum of intermediate goods, indexed by $i \in [0, \Lambda]$, is produced by firms operating under monopolistic competition. Each intermediate good is produced according to:

$$y_i(s^t) = q_i(s^t)\, l_i(s^t), \tag{9}$$

where $q_i(s^t)$ denotes the efficiency (productivity) of variety i and $l_i(s^t)$ denotes labor input.

The firm with the lowest marginal cost for each variety is the technological leader, earning monopoly rents through Bertrand competition against the second-best producer. Firms can operate multiple product lines simultaneously, expanding by innovating into additional varieties or contracting when losing technological leadership. Firms exit the market if they lose control of all their product lines. This structure generates endogenous firm dynamics through innovation and creative destruction, linking micro-level competition to macroeconomic productivity growth.[13]

3.5.1 Innovation by Incumbents

The productivity of each intermediate good evolves endogenously through innovation. Innovations arise when either an incumbent or a potential entrant successfully improves upon the existing technology for producing a given variety. When an innovation occurs for variety i, the new technological leader gains access to:

$$q_i(s^{t+1}) = (1+\sigma)\, \tilde{q}_i(s^t),$$

where $\tilde{q}_i(s^t)$ denotes the previous leader's technology level and $\sigma > 0$ is the innovation step size.

Incumbent firms can actively attempt to innovate and capture new product lines. Following the discrete-time version of Ates and Saffie (2021) based on Klette and Kortum (2004), a firm with

[13] Our quantitative results do not hinge on the specific Klette–Kortum structure. Any forward-looking endogenous growth model in which firms invest in innovation and creative destruction generates a similar link between firm values, innovation, and the trend. We adopt this framework because it can be disciplined using firm-level dynamics such as the distribution of firm sizes and exit rates.

n products can allocate research labor $L_r(s^t)$ to generate a per-product success probability:

$$x(s^t) = \xi \left(\frac{L_r(s^t)}{n} \right)^{\theta} \equiv \xi \left(l_r(s^t) \right)^{\theta},$$

where $l_r(s^t)$ denotes research labor per product.

The expansion and destruction of a firm's product portfolio follow binomial processes. Specifically, a firm with n products has probability:

$$\mathbb{B}(k, n, x(s^t)) = \binom{n}{k} x(s^t)^k (1 - x(s^t))^{n-k}, \tag{10}$$

of winning k new products through innovation, and probability:

$$\mathbb{B}(\tilde{k}, n, \Delta(s^t)) = \binom{n}{\tilde{k}} \Delta(s^t)^{\tilde{k}} (1 - \Delta(s^t))^{n-\tilde{k}}, \tag{11}$$

of losing $\tilde{k}$ products to creative destruction, where $\Delta(s^t)$ is the economy-wide creative destruction rate. Incumbent firms face a fixed innovation cost $F(s^t)$ per product line successfully innovated, which scales with the economy's size as $F(s^t) = A(s^t)F$.

Given these dynamics, the incumbent's value function with n products solves:

$$\begin{aligned} V_n(s^t) = \max_{x_n(s^t)} \; & n \left[\pi(s^t) - w(s^t) \alpha \left(\frac{x_n(s^t)}{\xi} \right)^{1/\theta} - (1 - \alpha) x_n(s^t) F(s^t) \right] \\ & + \mathbb{E} \left[m(s^{t+1}) \sum_{\tilde{k}=0}^{n} \mathbb{B}(\tilde{k}, n, \Delta(s^t)) \sum_{k=0}^{n} \mathbb{B}(k, n, x_n(s^t)) V_{n-\tilde{k}+k}(s^{t+1}) \Big| s^t \right]. \end{aligned} \tag{12}$$

Here $\pi(s^t)$ denotes per-product profits, $w(s^t)$ the wage, and $m(s^{t+1})$ the household's stochastic discount factor.

Because firms are atomistic, the two binomial processes (expansion and destruction) are independent, and transitions over firm size are separable. A firm with n products can thus transition within one period to any size in $[0, 2n]$.[14]

We also allow for a depreciation rate δ of each product line's technology, capturing gradual efficiency losses or evolving consumer preferences. Depreciation affects all producers symmet-

[14] See Appendix D for a detailed derivation of firm size distribution dynamics.

rically within a variety and thus does not alter the relative technology gap between leaders and followers.

3.6 Entry of New Firms

Firm entry is modeled analogously to incumbent innovation. Let $M(s^t) \in [0,1]$ denote the aggregate entrepreneurial effort directed toward starting new businesses. Entrepreneurs invest $\kappa M(s^t)$ units of labor and successfully create a new single-product firm in the next period with probability $M(s^t)^\nu$.

As with incumbent innovation, entry entails a fixed cost $F(s^t)$, which scales with the economy's size. Entrepreneurs choose $M(s^t)$ to maximize expected net returns:

$$\max_{M(s^t)} \left(M(s^t)\right)^\nu \mathbb{E}\left[m(s^{t+1})V_1(s^{t+1})\middle|s^t\right] - \alpha\kappa M(s^t)w(s^t) - (1-\alpha)\left(M(s^t)\right)^\nu F(s^t). \tag{13}$$

Here $V_1(s^{t+1})$ is the expected value of operating a single product line next period. The optimal solution $M^*(s^t)$ determines the endogenous entry rate of new firms. Together with incumbent innovation, entry shapes the creative destruction rate and thus the economy's long-run growth dynamics.

3.7 Equilibrium Characterization

The parsimony of the model enables a clear mapping between interest rate volatility, firm innovation, and the endogenous evolution of productivity.

Household Discounting. The household stochastic discount factor is:

$$m(s^t, s^{t+1}) = \beta \frac{C(s^{t+1})^{-\gamma}}{C(s^t)^{-\gamma} - \phi\mu(s^t)}. \tag{14}$$

Here $\mu(s^t)$ is the Lagrange multiplier on the collateral constraint (3). The collateral constraint affects discounting through the wedge $\mu(s^t)$, because binding constraints raise the marginal value of relaxing borrowing limits and increase the effective discount rate applied to future firm payoffs.

Intermediate Good Production. Intermediate good producers face a unit-elastic demand curve:

$$y_i(s^t) = \frac{Y(s^t)}{\Lambda p_i(s^t)}, \tag{15}$$

where $p_i(s^t)$ is the price of variety i. Under Bertrand competition, per-product profits and labor demand become independent of the variety-specific productivity $q_i(s^t)$. Specifically:

$$\pi(s^t) = \frac{\sigma}{1+\sigma}\frac{Y(s^t)}{\Lambda}, \tag{16}$$

$$l(s^t) = \frac{Y(s^t)}{\Lambda w(s^t)(1+\sigma)}. \tag{17}$$

Because firm-level decisions are independent of individual q_i, firm value is proportional to the number of products: $V_n(s^t) = nV_1(s^t)$.

Firm Value and Innovation. Given proportionality, the value of controlling a single product line satisfies:

$$V_1(s^t) = \max_{x(s^t)} \left\{ \pi(s^t) - w(s^t)\alpha \left(\frac{x(s^t)}{\xi}\right)^{1/\theta} - (1-\alpha)x(s^t)F(s^t) + \mathbb{E}\left[m(s^t, s^{t+1}) \left(1 - \Delta(s^t) + x(s^t)\right) V_1(s^{t+1}) \middle| s^t \right] \right\}. \tag{18}$$

The optimal incumbent innovation effort per product line is:

$$x^*(s^t) = \left[\frac{\theta}{\alpha} \xi^{1/\theta} \frac{\mathbb{E}\left[m(s^t, s^{t+1}) V_1(s^{t+1}) - (1-\alpha)F(s^t) \mid s^t \right]}{w(s^t)} \right]^{\theta/(1-\theta)}. \tag{19}$$

Similarly, the mass of new entrant firms is:

$$M^*(s^t) = \left[\frac{\nu}{\alpha\kappa} \frac{\mathbb{E}\left[m(s^t, s^{t+1}) V_1(s^{t+1}) - (1-\alpha)F(s^t) \mid s^t \right]}{w(s^t)} \right]^{1/(1-\nu)}. \tag{20}$$

In equilibrium, incumbent innovation and entry jointly pin down the creative destruction rate, and movements in discounting and in the normalized value of future firm payoffs propagate into $\Delta(s^t)$ through (19) and (20).

Productivity Growth. The aggregate creative destruction rate combines entry and incumbent innovation:

$$\Delta(s^t) = \frac{(M^*(s^t))^\nu}{\Lambda} + x^*(s^t). \tag{21}$$

Aggregate output evolves according to:

$$Y(s^t) = e^{z(s^t)} A(s^t) l(s^t), \tag{22}$$

where $A(s^t)$ is the endogenous productivity index:

$$\ln A(s^t) = \frac{1}{\Lambda} \int_0^\Lambda \ln q_i(s^t)\, di. \tag{23}$$

The law of motion for productivity satisfies:

$$\ln(A(s^t, s^{t+1})) - \ln(A(s^t)) = \Delta(s^t) \ln(1+\sigma) + \ln(1-\delta). \tag{24}$$

Productivity growth can be negative if creative destruction is insufficient to offset depreciation. The endogenous productivity index $A(s^t)$ corresponds to the common stochastic trend estimated in Section 2: changes in $A(s^t)$ map into persistent changes in the levels of GDP, consumption, and investment.

Labor Market and Wage Determination. Combining (22) and (17), the equilibrium wage satisfies:

$$w(s^t) = \frac{e^{z(s^t)} A(s^t)}{\Lambda(1+\sigma)}. \tag{25}$$

Household Optimality Conditions. The household's first-order conditions are:

$$C(s^t)^{-\gamma} = \mu(s^t) + \beta \hat{R}(s^t)\, \mathbb{E}\left[C(s^{t+1})^{-\gamma} \mid s^t \right], \tag{26}$$

$$C(s^t) + \hat{q}(s^t) B^H(s^t) \leq w(s^t)\bar{L} + B^H(s^{t-1}) + \Lambda e(s^t) - \kappa \alpha M(s^t) w(s^t) - (1-\alpha)(M(s^t))^\nu F(s^t), \tag{27}$$

where $e(s^t)$ captures firm net earnings per product, derived from (18). The collateral constraint remains:

$$\hat{q}(s^t)B^H(s^t) \geq -\phi\Lambda V_1(s^t), \tag{28}$$

where $V(s^t) = \Lambda V_1(s^t)$ is the total collateral value.

Stationarity and Solution. Appendix E renders the model stationary by normalizing growing variables by the productivity index $A(s^t)$ and summarizes the full system of stochastic equilibrium conditions.

3.8 Trend Dynamics and Interest Rates

Equation (24) shows that stationary distortions affecting the endogenous creative destruction rate $\Delta(s^t)$ can generate permanent shifts in the level of the productivity index $A(s^t)$, defined in (23). Since $A(s^t)$ governs the long-run level of the economy, fluctuations in $\Delta(s^t)$ generate hysteresis in output and consumption. In this class of models, stationary shocks can thus produce low-frequency (trend) dynamics through internal propagation.

Understanding these endogenous trends requires analyzing how aggregate shocks affect the determinants of creative destruction—firm entry and incumbent innovation decisions, characterized by (19) and (20). Two endogenous objects mediate this transmission: (i) the household's stochastic discount factor, and (ii) the expected future value of a product line relative to the current wage.

Effects of TFP Shocks. Consider first a TFP shock, $z(s^t)$. As our model is a small open economy facing an exogenous interest rate, TFP shocks have little effect on intertemporal discounting in unconstrained states. Meanwhile, equation (25) shows that a positive TFP shock raises wages, which increases the denominator of the normalized value of future firm payoffs. At the same time, profits and innovation costs scale with aggregate activity. As a result, when the collateral constraint is slack, TFP shocks generate limited movements in the normalized incentives that govern $x^*(s^t)$

and $M^*(s^t)$.[15]

When a sufficiently adverse TFP realization pushes the economy into the constrained region, however, the Fisherian deflation channel becomes operative: falling asset values tighten the borrowing constraint, raise the marginal value of relaxing borrowing limits (via $\mu(s^t)$), and depress firm values and innovation incentives. In this case, TFP shocks can have persistent effects on the trend by triggering binding financial constraints.

Effects of Interest Rate Shocks. By contrast, shocks to the international borrowing rate faced by households directly affect discounting without necessarily changing contemporaneous firm profits or innovation costs.[16] An increase in financing costs raises the gross borrowing rate $\hat{R}(s^t)$ and, through (26)–(14), increases the effective discount rate applied to future firm payoffs. Lower firm values reduce collateral, tighten borrowing limits when constraints are relevant, and depress innovation and entry incentives via (19) and (20).

Collateral Constraints and Amplification. Both TFP and interest rate shocks can influence trend growth through collateral constraints. When the borrowing constraint (28) binds, households are forced to delever, lowering current consumption and raising the marginal value of relaxing borrowing limits. This reduces firm values, tightens borrowing conditions further, and can trigger a Fisherian spiral. Accordingly, large adverse shocks, especially those that move the economy into the constrained region, can have persistent effects on the trend through endogenous movements in $\Delta(s^t)$.

The Role of Volatility Shocks. Finally, even absent realized interest rate shocks, volatility shocks matter. Consider a state in which the borrowing constraint is slack. An increase in interest rate volatility, $\sigma_R(s^t)$, raises the likelihood of large future movements in the borrowing rate. Because the collateral constraint is occasionally binding, the effects of future tightening and easing are not symmetric: large rate hikes can sharply reduce firm values and push the economy into the

[15] A fixed resource cost F (paid in goods rather than labor) breaks exact scale invariance, since it does not scale one-for-one with wages and aggregate activity. Quantitatively, this effect is small in our calibration and is most relevant when x and M are already low (i.e., near or inside the constrained region), where F can contribute to amplification by further compressing cash flows and firm values.

[16] We abstract from working capital constraints, which would otherwise transmit interest rate shocks into wages and operating costs. With working capital frictions, interest rate shocks would affect wages similarly to TFP shocks with, therefore, limited additional effects on growth.

constrained region, while large cuts cannot further relax an already slack constraint. As a result, higher volatility lowers expected firm values and reduces innovation and entry incentives today, even holding fixed the conditional mean of interest rates. This effect is stronger in economies that spend more time near the constrained region, because volatility raises the probability of entering states in which the Fisherian amplification mechanism is operative.

4 Quantitative Analysis

In this section, we show that the model replicates the differential sensitivity of the productivity trend to interest rate volatility in emerging and advanced economies. We first calibrate the model to Mexico. We then construct an advanced economy calibration by changing only the parameters that govern financial frictions, pledgeability and the pricing of external borrowing, while keeping all other parameters and all shock processes common across the two economies. We show that a volatility shock generates a much larger and more persistent decline in the productivity trend in the emerging economy calibration, consistent with the evidence in Section 2, and these impulse responses are not targeted in the calibration. We then explain how our model generates this result. To give the intuition up front, when the collateral constraint is slack, volatility mainly operates through a risk and discounting channel with relatively linear effects. When, however, low productivity pushes the economy into the constrained region, volatility triggers a Fisherian collateral mechanism that amplifies deleveraging and depresses firm values, innovation, and the endogenous trend. Finally, we quantify the sources of the emerging versus advanced gap by separating the role of pledgeability from the role of spreads, and we illustrate the implications for average trend dynamics and cross-country dispersion over the recent global volatility cycle.

4.1 Calibration: Heterogeneous Financial Frictions

We calibrate the model to match key features of Mexico at a quarterly frequency. The model has 21 parameters. We split them into two groups. The first group consists of 11 parameters that we either take from standard values in the literature or estimate directly. Table 1 reports these values. We estimate the U.S. real interest rate process and its stochastic volatility as described in Appendix A.1. We set the average interest rate to 4% per year (Mendoza, 1991), which corre-

sponds to roughly 1% per quarter. We set the TFP process parameters (ρ_z, η_z) following Neumeyer and Perri (2005). We set the innovation curvature parameters for incumbents and entrants to 0.5 (Akcigit and Kerr, 2018). We assume CRRA utility with curvature $\gamma = 2$, a standard choice in quantitative Sudden Stop models. Finally, we set the depreciation rate of ideas to $\delta = 0.015$ per quarter. This implies that, in the absence of innovation and entry, the efficiency index shrinks at 1.5% per quarter. This magnitude is consistent with the lower tail of our estimated trend growth distribution for emerging economies.

Table 1: Externally Calibrated Parameters

Parameter	Symbol	Value	Source
Average U.S. Interest Rate	$\bar{R}$	$(1.04)^{0.25} - 1$	Mendoza (1991)
Persistence of Interest Rate	ρ_R	0.91	Estimation, U.S. data
Average Interest Rate Volatility	μ_σ	0.17	Estimation, U.S. data
Persistence of Interest Rate Volatility	ρ_σ	0.94	Estimation, U.S. data
Volatility of Interest Rate Volatility	η_σ	0.12	Estimation, U.S. data
Persistence of TFP Shock	ρ_z	0.95	Neumeyer and Perri (2005)
Volatility of TFP Shock	η_z	0.02	Neumeyer and Perri (2005)
Innovation Curvature Cost by Incumbents	θ	0.50	Akcigit and Kerr (2018)
Innovation Curvature Cost by Entrants	υ	0.50	Akcigit and Kerr (2018)
Utility Function Curvature	γ	2	Standard
Depreciation of Ideas	δ	0.015	Estimation, lower tail of trend growth

Notes: This table reports externally calibrated parameters, their symbols, numerical values, and data or literature sources. Interest rate and volatility parameters are estimated using U.S. data as described in Appendix A.1.

The second group consists of 10 internally calibrated parameters, summarized in Table 2. We set the step size σ to 0.22 to match an average annualized growth rate of about 2%, consistent with Neumeyer and Perri (2005). We set the entry cost κ to 31 to generate an annualized entry rate of 10%.[17] We set the R&D cost level ξ to 0.49 so that the average incumbent firm size relative to entrants is 3. For the cost structure of innovation, we set $\alpha = 0.8$ so that labor accounts for two-thirds of total R&D costs (Moris and Shackelford, 2020), and we set $F = F(s^t)/A(s^t) = 0.21$ so that total innovation and product-creation expenditures (entry and incumbent expansion) amount to approximately 4 percent of GDP, consistent with estimates of broad intangible investment for Mexico (Valdivia López and Borrayo López, 2023).[18] We normalize the mass of products to $\Lambda = 3$, ensuring a unit mass of firms along the balanced growth path. We set the discount factor $\beta = 0.98$

[17] INEGI, Mexico's national statistical office, reports a monthly establishment birth rate of 0.81% in its Business Demography Survey (EDN 2021). Annualizing this rate yields roughly 9.7%, which we round to 10% for calibration. See Instituto Nacional de Estadística y Geografía (INEGI) (2021).

[18] Firm-level evidence on revenues from new products (INEGI and CONACYT, 2019) and data on startup costs (World Bank, 2020) imply magnitudes of fixed outlays that are consistent with this calibration, providing external validity for the value of F.

to match Mexico's long-run external position, targeting an external debt to GDP ratio close to 33% annually, in line with Lane and Milesi-Ferretti (2017). We set the collateral coefficient ϕ to 0.62 so that the model produces an annual crisis probability close to 3%, consistent with the Sudden Stops literature.[19] We set $\iota_0 = 0.01$, the parameter governing the average spread charged by the representative financial intermediary, to match a 1% quarterly spread in line with Mexico's average EMBI spread between 1994 and 2019. Finally, we set $\iota_1 = 14.58$ to match the sensitivity of Mexico's EMBI spread to volatility during the Great Recession.[20]

Table 2: Internally Calibrated Parameters

Parameter	Symbol	Value	Main Identification	Target
Step Size	σ	0.22	Annual Growth Rate	2%
Cost Level Entry	κ	31	Annual Entry Rate	10%
Cost Level R&D	ξ	0.49	Avg. Firm Size Relative to Entrants	3
Variable Cost Share R&D	α	0.80	R&D Wage Bill to Total R&D Costs	2/3
Fixed Cost R&D	F	0.21	Total R&D Costs to Firm Value	5%
Mass of Products	Λ	3	Unit Mass of Firms	N/A
Discount Factor	β	0.98	Annual Debt-to-GDP Ratio	33%
Borrowing Constraint	ϕ	0.62	Annual Prob. of Crisis	3%
Financial Intermediary Average Price	ι_0	0.01	Average Spread	1%
Financial Intermediary Price Sensitivity	ι_1	14.58	Spread Sensitivity	$\frac{\text{Spread}_{09Q1} - \text{Spread}_{08Q1}}{\sigma_{09Q1} - \bar{\sigma}}$

Notes: This table reports internally calibrated parameters, their symbols, values, main identification roles, and calibration targets. All parameters are calibrated using the Mexico benchmark. The advanced economy calibration changes only ϕ, ι_0, and ι_1 while keeping all other parameters fixed.

Due to the nonlinear nature of a model with an occasionally binding borrowing constraint, we solve the model using global methods. We employ a hybrid method that combines time iteration with value function iteration. Appendix F provides a detailed description of the solution method.

To highlight the importance of heterogeneous financial frictions, we construct an advanced economy calibration by changing only three parameters from Table 2, namely ϕ, ι_0, and ι_1, and keeping all other parameters and all shock processes fixed. We set $\phi = 0.92$ so that the economy experiences a financial crisis with roughly half the baseline probability, around 1.5% per year, consistent with targets used for developed economies (Bianchi and Mendoza, 2020). We set $\iota_0 = 0.002$ and $\iota_1 = 2.16$ so that the average quarterly spread is 0.25% and the spread sensitivity to U.S. interest rate volatility is consistent with what was observed for a panel of advanced economies during

[19] We define a crisis or Sudden Stop as an event in which the current account to GDP ratio is two standard deviations above its long-run mean and the borrowing constraint binds, following (Mendoza, 2010; Bianchi et al., 2016).

[20] Mexico's annual EMBI spread increased by 2.5 percentage points between 2008Q1 and 2009Q1. The associated spike in U.S. real interest rate volatility, relative to trend, was close to 20%. We map this increase to our stochastic volatility grid. This implies $\iota_1 = \frac{\Delta \text{Spread}}{\Delta \sigma} \approx \frac{0.006}{0.0004}$.

the Great Recession.[21] Only ϕ, ι_0, and ι_1 differ between the emerging and advanced economy calibrations.

4.2 Model Meets Data: Stochastic Volatility and Endogenous Trend Dynamics

We use the main empirical fact described in Section 2 to assess the quantitative implications of the calibrated model. We compute generalized impulse response functions (GIRFs) from model-simulated data, following Koop et al. (1996). The shock is a one standard deviation increase in the volatility of the world interest rate, the model analogue of the U.S. real interest rate. We compute the response of the accumulated productivity trend by simulating two economies that share the same sequence of shocks, one with a volatility shock in period T and one without, and taking the difference between the two paths. We repeat this exercise 10,000 times and average across simulations.[22]

Figure 4 reports the impulse responses of the accumulated trend for the baseline and advanced calibrations. Two patterns emerge. First, the advanced economy calibration exhibits a substantially smaller decline in the productivity trend than the baseline calibration. Second, the heterogeneity between the baseline and advanced economy calibration is qualitatively and quantitatively in line with our empirical findings. As these impulse responses are not targeted in the calibration and they provide an out-of-sample check on the model suggesting that the uncertainty induced forces weighting on growth are in the right ballpark.[23]

[21] To set ι_1 we calculate the change in five-year mean CDS spreads, relative to the United States, between 2008 and 2009 for a group of advanced economies. We follow a process identical to the one described for our baseline calibration. Our sample includes Belgium, Denmark, Finland, France, Germany, Italy, Netherlands, Norway, Portugal, Spain, Sweden, and the United Kingdom. Our data were obtained from Markit.

[22] Each simulation lasts 390 quarters. We discard the first 350 quarters to remove dependence on initial conditions. For each draw, we use the same underlying sequence of shocks across the treated and control economies, and we use the same shock sequences for the baseline and advanced calibrations.

[23] Given the pricing formulation in Equation (7), a volatility shock also induces a level component in the interest rate faced by households. Appendix C isolates the effect of a pure change in interest rate volatility and shows that volatility itself accounts for roughly 30% of the total response.

Figure 4: Trend Growth Rate Impulse Response Functions to a World Interest Rate Volatility Shock

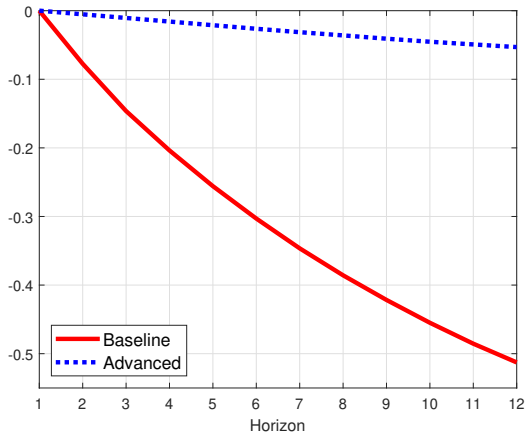

Notes: This figure presents impulse response functions of the accumulated productivity trend to a one standard deviation stochastic volatility shock of the world interest rate, for the baseline (red solid line) and advanced (blue dotted line) model calibrations. Responses are computed from model-simulated data using the generalized impulse response procedure described in Section 4.2.

4.3 Mechanism: Constraints, Volatility, and Asymmetry

The GIRFs show that a volatility shock has much larger effects on the productivity trend in the emerging economy calibration. In this subsection we delve into the reasons behind this difference. The key object is the interaction of aggregate productivity Z and interest rate volatility σ_R with the collateral constraint. Low productivity realizations move the economy into states in which the constraint binds. In those states, volatility shocks trigger a Fisherian collateral mechanism that amplifies deleveraging and depresses firm values and innovation incentives in addition to any other effects. When the constraint is slack, volatility mainly operates through a risk and discounting channel with relatively symmetric effects (in absolute value) between increases and decreases.

4.3.1 Policy functions and the constrained region

Figure 5 summarizes these forces using policy functions. Panel (a) plots the endogenous trend growth rate g as a function of σ_R for three values of Z. Volatility reduces trend growth at all productivity levels, but the decline is much larger when productivity is low. Panel (b) explains this state dependence. It plots the Lagrange multiplier on the collateral constraint, $\tilde{\mu}$, as a function of σ_R. The multiplier measures the tightness of the borrowing constraint. When productivity is at

or above its average level, we have that $\tilde{\mu} = 0$ for all values of σ_R, so volatility does not tighten the constraint. When productivity is sufficiently low, higher volatility increases $\tilde{\mu}$ sharply, pushing the economy deeper into the constrained region.

Panel (c) plots $\tilde{\mu}$ as a function of Z for different levels of volatility. As productivity falls below its long-run mean, the constraint starts binding, and the severity of this tightening depends on σ_R. For a given decline in Z, higher volatility implies a larger multiplier and a sharper contraction in borrowing capacity. As a result, the same productivity realization can generate very different innovation and growth outcomes depending on the volatility state. This state dependence is central for understanding why volatility shocks have limited effects in normal times but large effects when the economy visits low productivity states.

Figure 5: Policy Functions: Volatility, Financial Constraints, and Trend Growth

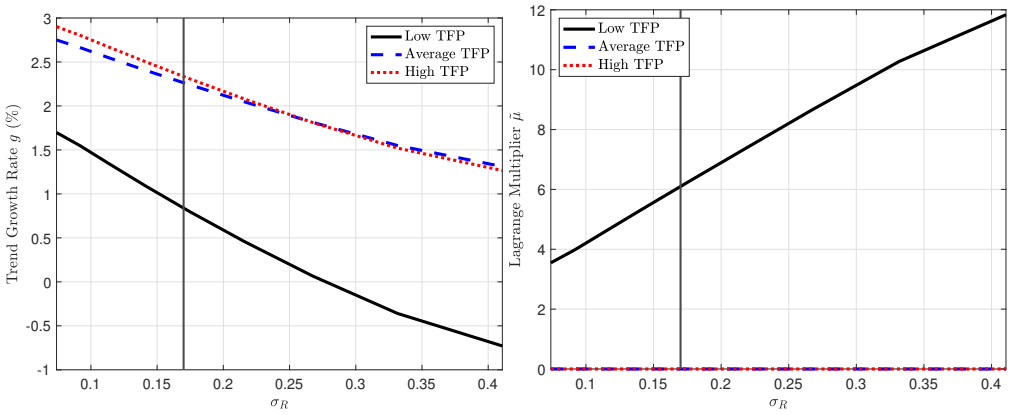

(a) Trend Growth Rate and Volatility

(b) Lagrange Multiplier and Volatility

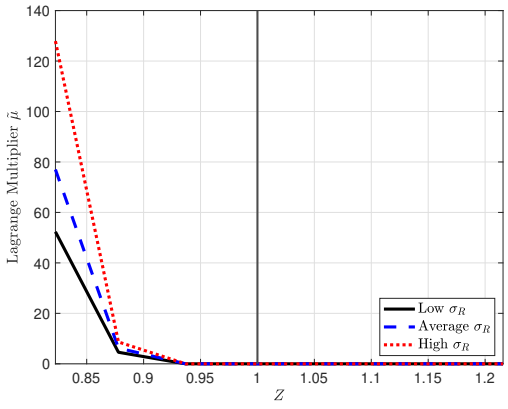

(c) Lagrange Multiplier and Productivity

Notes: This figure plots policy functions for the endogenous trend growth rate, g, and the Lagrange multiplier on the borrowing constraint, $\tilde{\mu}$. Vertical lines denote ergodic means of interest rate volatility and TFP. Trend growth rates are annualized. Bond holdings and the interest rate are fixed at their long-run means.

4.3.2 Asymmetry response to symmetric interest rate shocks

Another implication of the occasional binding constraint is that a more volatile interest rate environment can lower expected firm values and trend growth even when interest rate innovations are symmetric on average. When volatility is higher, interest rate innovations are larger in absolute value, conditional on hikes or cuts.[24] Near the constrained region, the real effects of hikes and cuts of the same absolute size need not be symmetric. When the collateral constraint binds, an interest rate hike tightens borrowing capacity and triggers a Fisherian feedback through collateral values. When the interest rate falls, the relaxation is weaker because the multiplier is bounded below by zero. As a result, a high-volatility environment, which makes large interest rate movements more likely, lowers the expected value of firms and reduces innovation and entry incentives, even in the absence of a contemporaneous first-moment shock.

In contrast, when the constraint rarely binds, the main nonlinearity comes from discounting. Since the discount factor is concave in the interest rate, Jensen's inequality implies that hikes can have smaller absolute effects on discounting than cuts of the same magnitude. This can attenuate asymmetry, and for sufficiently large shocks it can generate a mild reversal.[25]

To quantify asymmetry, we compute impulse responses to symmetric interest rate shocks using an approach similar to a generalized impulse response function. We vary the magnitude of the shock while maintaining symmetry, meaning equal absolute sizes for hikes and cuts. Each simulation lasts 390 quarters, we discard the first 350 quarters, and we repeat the exercise 5,000 times for each shock size. We compute the average impact response for the baseline and advanced calibrations when the interest rate shock materializes, using the same underlying shock sequences across calibrations.[26]

Figure 6 summarizes the results. Panel A reports an asymmetry statistic for the trend growth response, defined as the absolute impact response to a hike minus the absolute on-impact response to a cut, with responses standardized by the long-run standard deviation of g. Interest rate shocks

[24] Let the interest rate innovation be $\omega(s^t)\sigma(s^t)$ with $\omega(s^t) \sim N(0,1)$. Conditional on a hike, $\mathbb{E}[\omega(s^t)\sigma(s^t) \mid \omega(s^t) > 0, s^t] = \sigma(s^t)\frac{\phi(0)}{1-\Phi(0)}$, and the same logic applies to cuts.

[25] This Jensen effect is dominated when the economy frequently visits constrained states, but it can be visible in the advanced calibration when the constraint binds less often.

[26] The response of g declines monotonically after the first period of the shock, so the impact response constitutes also the max response.

are expressed in standard deviations relative to the average level of interest rate volatility. Panel B reports, for each shock size, the probability that the absolute interest rate change exceeds that threshold under two volatility regimes, a low-volatility state one standard deviation below the mean and a high-volatility state one standard deviation above the mean.

Figure 6: Asymmetry in Impulse Responses to Symmetric Interest Rate Shocks

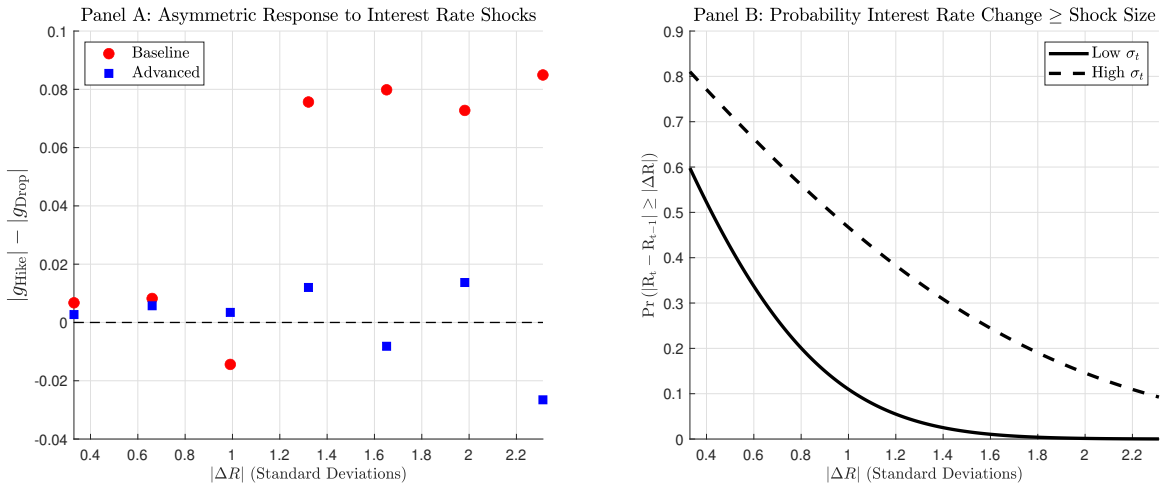

Notes: The asymmetry in responses is presented as $|g^{\text{Hike}}| - |g^{\text{Cut}}|$, where g^{Hike} (g^{Cut}) corresponds to the on-impact response of the trend growth rate g (standardized with respect to its long-run mean and standard deviation) to an interest rate hike (cut). Interest rate shocks are expressed in standard deviations. Low (High) σ_R corresponds to interest rate volatility that is one standard deviation below (above) its long-run average.

Figure 6 reveals two patterns. First, for the emerging market economy asymmetry clearly increases with shock size. For small shocks, the responses to hikes and cuts are similar, but for larger shocks the absolute response to a hike exceeds the absolute response to a cut. Second, asymmetries are mainly present in the baseline calibration. The advanced economy calibration exhibits no clear asymmetries, consistent with the discounting force discussed above.

Panel B shows that the shock sizes for which asymmetries arise are much more likely when volatility is high. For example, an increase in the real interest rate of at least one standard deviation occurs with about 10% probability in the low-volatility regime, but with almost 50% probability in the high-volatility regime. Taken together, the two panels imply that higher volatility increases the probability mass on shocks for which the economy's responses are strongly asymmetric. This lowers expected growth in the baseline calibration, and leads households to reduce current consumption and increase precautionary savings, generating an immediate decline in the endogenous trend even in the absence of a first-moment shock.

To isolate the role of stochastic volatility in long-run moments, we also consider an economy in which the standard deviation of the world interest rate is fixed at its ergodic mean. Table 3 reports selected long-run moments for the baseline and advanced calibrations under stochastic volatility and under deterministic volatility.

Table 3: Volatile Rates and Volatile Trends: Deterministic Volatility

Moment	Baseline		Advanced	
	SV	No SV	SV	No SV
$\sigma(g)/\mathbb{E}(g)$	0.18	0.13	0.11	0.12
$\sigma(CA/Y)$ %	3.08	2.92	1.11	0.91
$\mathbb{E}(B^H/Y)$ %	-32.49	-33.83	-54.05	-54.23
Spread %	1.00	1.00	0.25	0.25
Prob. Sudden Stop %	2.68	3.23	1.61	1.60

Notes: SV denotes the scenario with stochastic volatility in the world interest rate. In the No SV case, the volatility process is shut down and the standard deviation of the world interest rate is fixed at its long-run (ergodic) mean. All moments are computed from long simulated samples under each regime.

For the baseline calibration, shutting down stochastic volatility reduces the coefficient of variation of trend growth by roughly 30%. For the advanced calibration, the volatility of trend growth changes little. Both economies experience lower current account volatility when volatility shocks are removed, reflecting reduced precautionary savings motives and a smoother consumption path. In the baseline calibration, the absence of volatility also encourages higher external borrowing and increases exposure to Sudden Stops, as reflected in their higher probability.[27] These results indicate that stochastic volatility is a key driver of trend dynamics in the baseline calibration, and that its effects depend on financial frictions. We next separate the contributions of pledgeability and spreads.

4.4 Interest Rate Risk and Financial Frictions

The mechanism we have been highlighting depends on two features of the emerging economy calibration: limited pledgeability and higher borrowing costs. In this subsection, we separate the role of collateral tightness from the role of spreads. We construct an intermediate calibration that we call the relaxed constraint economy. It is identical to the baseline calibration except that we set

[27] Our Sudden Stop definition uses a current account to GDP threshold defined relative to each economy's own long-run distribution, and the distribution changes across calibrations. As a result, differences in crisis probabilities reflect both differences in financial tightness and changes in equilibrium borrowing and current account volatility.

the collateral coefficient ϕ to its advanced-economy value, while keeping the spread parameters (ι_0, ι_1) at their baseline values. Comparing the baseline and relaxed constraint economies isolates the role of pledgeability. Comparing the relaxed constraint and advanced economies isolates the role of spreads.

Table 4 reports long-run moments for the three economies. Relaxing the borrowing constraint has large effects on volatility. The coefficient of variation of trend growth declines by 22%, and current account volatility falls by half.. In terms of the emerging versus advanced gap in trend volatility, the change in pledgeability accounts for roughly 60% of the difference, with the remaining share attributed to spreads. Sudden Stop probabilities need not move monotonically across calibrations because they are equilibrium outcomes that reflect endogenous borrowing, precautionary savings, and the distribution of current account fluctuations.[28]

Table 4: Financial Frictions and Business Cycles

Moment	Baseline	Relaxed Constraint	Advanced
$\mathbb{E}(\text{Spread})$ %	1.00	1.00	0.25
$\sigma(g)/\mathbb{E}(g)$	0.18	0.14	0.11
$\sigma(CA/Y)$ %	3.08	1.49	1.11
$corr(\text{Domestic Spread}, g)$	-0.54	0.49	0.49
Prob. Sudden Stop %	2.68	1.50	1.61
$\mathbb{E}(B^H/Y)$ %	-32.49	-52.80	-54.05

Notes: This table reports long-run simulated moments for three calibrations: the baseline, the relaxed constraint economy (same as baseline except for ϕ set to its advanced-economy value), and the advanced economy (baseline with higher pledgeability and lower, less volatility-sensitive spreads). All moments are computed under stochastic volatility in the world interest rate.

We also report the correlation between the domestic spread and trend growth. Standard small open economy models often assume that spreads and productivity are negatively correlated (Neumeyer and Perri, 2005). In our model, this relationship is endogenous and depends on the degree of financial tightness. In the baseline calibration, domestic spreads are strongly countercyclical with respect to trend growth, while in the relaxed constraint and advanced calibrations the correlation becomes positive.[29]

A key implication of the baseline calibration is the presence of Sudden Stops. These episodes

[28] We also find excess consumption volatility (with respect to output) in our baseline calibration. Not surprisingly, we find that the excess volatility decreases as financial constraints are relaxed. Similar patterns are observed for the current account-to-GDP and trade balance-to-GDP ratios.

[29] We define the domestic spread as the difference between the domestic interest rate and the rate charged by intermediaries, $\mathbb{E}\left[R^B(s^{t+1}) - \hat{R}(s^t)\right] = \mu(s^t)/\mathbb{E}[\lambda(s^{t+1}) \mid s^t]$.

involve sharp reversals in the current account together with severe contractions in consumption and output. They arise from occasionally binding collateral constraints and endogenous collateral values, which activate a Fisherian deflation mechanism during periods of financial stress (Mendoza, 2005, 2010). Unlike business cycle fluctuations with exogenous growth, Sudden Stops in our model have persistent effects on productivity and output. Appendix G presents event studies for the baseline calibration and highlights the persistence of the trend and slow recoveries after crises. This persistence is consistent with models that integrate financial frictions into growth dynamics (Queralto, 2020; Guerron-Quintana and Jinnai, 2019) and with the hysteresis documented in the empirical literature (Cerra and Saxena, 2008).

4.5 Volatile Rates and Fragile Growth

We next study the economic magnitude of the mechanism over the recent global volatility cycle. We use the observed path of the U.S. real interest rate and its volatility (Figure 11 in Appendix A.1). We draw 10,000 TFP sequences and feed each sequence, together with the observed interest rate and volatility paths, into the three calibrations. Since all economies face the same realizations of global rates and volatility and the same TFP process, differences in outcomes reflect internal propagation through financial frictions.

Figure 7 reports average deviations from deterministic trends for productivity and for the multiplier on the borrowing constraint. Panel (a) shows that the three economies follow markedly different average trend deviations over the sample. During the low-volatility period with declining interest rates between 1990 and 2006, emerging markets grew substantially faster than their average rate, while the advanced economies gained little by this metric. By 2006, the baseline economy is about 4% above trend. After 2006, when global risk rises, these gains are reversed. By 2018, the baseline economy is nearly 2% below trend, while the relaxed constraint and advanced economies experience substantially smaller declines.

Panel (b) links these outcomes to financial constraints.[30] The reversal in the baseline economy coincides with a sharp increase in the multiplier, reflecting tight borrowing conditions and

[30]The figure reports average deviations across 10,000 TFP paths. We measure $\ln A_t - \ln \bar{A}_t$ with $A_t = \prod_{i=0}^{t}(1+g_i)$ and $\bar{A}_t = (1+\bar{g})^t$, where $\bar{g}$ is the ergodic mean of g. For the multiplier we report percentage deviations from its deterministic counterpart, with $\mu_t = A_t^{-\gamma}\tilde{\mu}_t$ and $\bar{\mu}_t = \bar{A}_t^{-\gamma}\bar{\tilde{\mu}}$. Appendix H presents a similar exercise for the Lagrange multiplier in levels and the probability of a binding borrowing constraint.

a deleveraging episode. The relaxed constraint and advanced economies display much smaller movements in the multiplier. In the baseline calibration, the Fisherian feedback is strong enough that the economy tends to keep more precautionary slack in normal times, but when adverse volatility and productivity realizations push it into the constrained region, the tightening is abrupt and persistent. In the relaxed constraint and advanced calibrations, the economy is less exposed to these amplification dynamics, so increases in global risk lead to milder deleveraging and smaller trend losses.[31]

Figure 7: Deviations from Trend Based on Actual Interest Rate and Volatility Time Series

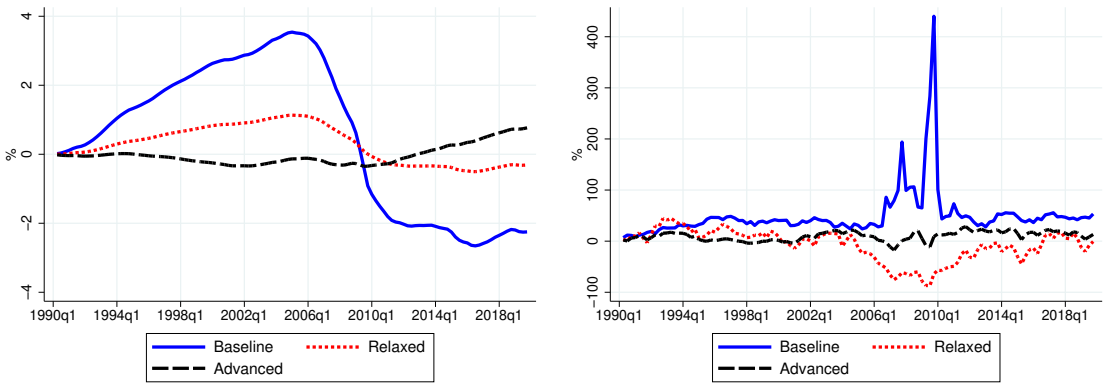

(a) $\ln A_t - \ln \bar{A}_t$ (b) $\frac{\mu_t - \bar{\mu}_t}{\bar{\mu}_t}$

Notes: This figure shows, for the three calibrations (baseline, relaxed constraint, advanced), the average deviation of productivity and of the Lagrange multiplier from their deterministic trends when all economies are subjected to the same path of U.S. real interest rates and volatility. Panel (a) reports $\ln A_t - \ln \bar{A}_t$; panel (b) reports percentage deviations of the multiplier from its deterministic counterpart. Averages are taken across 10,000 simulated TFP paths.

To connect these average outcomes to cross-sectional dynamics, Figure 8 reports the average and dispersion of the trend growth rate g across the 10,000 simulated economies. We construct these series following the same approach as in Section 2.5 and focus on the same sample window. Panel (a) shows that average trend growth in the baseline economy falls sharply during high-volatility episodes. Panel (b) shows that dispersion in g rises substantially for the baseline economy and remains much smaller for the relaxed constraint and advanced calibrations. This pattern mirrors the empirical evidence and highlights that the same global volatility cycle can

[31] The global risk shock in this experiment is stochastic volatility in the *U.S.* interest-rate process. Consequently, episodes in which emerging-market risk premia rose for reasons largely orthogonal to uncertainty about U.S. rates (e.g., the 1997–98 Asian/Russian crises) need not appear as large realizations of the shock in Figure 7. In the model, such episodes would be better represented by an increase in the country spread (or by feeding in a broader measure of global financial risk/uncertainty rather than U.S.-rate volatility).

generate both lower average growth and higher dispersion in emerging markets.

Figure 8: Average and Dispersion of Trend Growth

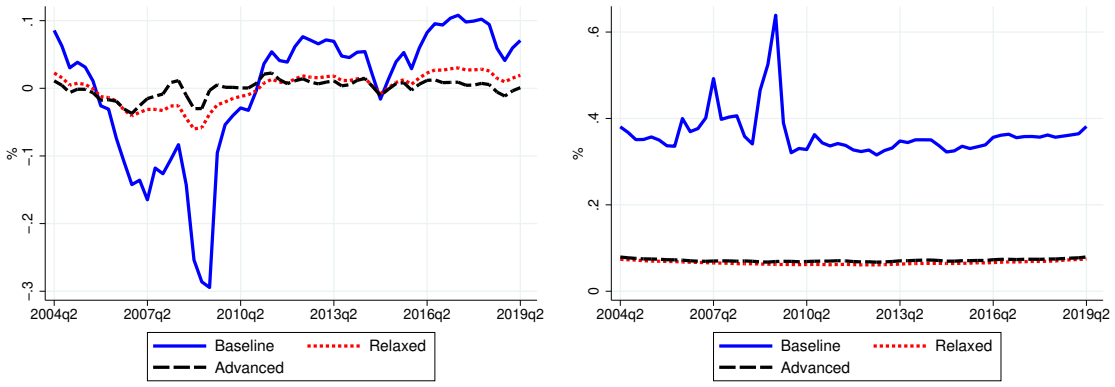

(a) Growth Rate g – Average

(b) Growth Rate g – Standard Deviation

Notes: For each quarter in the sample window, we compute the cross-sectional average and standard deviation of the trend growth rate g across simulated economies, using the same sample window and construction as in Section 2.5. Panel (a) reports the cross-sectional average; panel (b) reports the cross-sectional standard deviation, for the baseline, relaxed constraint, and advanced calibrations.

Figure 9 isolates the role of stochastic volatility in these dynamics for the baseline calibration. We repeat the exercise in Figure 8 under two counterfactual scenarios, one in which the interest rate level is fixed at its mean while volatility follows its stochastic process, and one in which volatility is fixed at its mean while the interest rate follows its stochastic process. The decomposition shows that aggregate risk is the primary driver of both the decline in average trend growth and the rise in dispersion. When interest rate volatility is held fixed at its mean, the collapse in average growth and the increase in dispersion largely disappear.

The remaining question is why the same panel of productivity shocks generates much larger dispersion in trend growth for emerging markets than for advanced economies. Figure 10 links dispersion to the interaction between volatility and the constrained region of the state space. The figure plots, for each calibration, the difference in the trend-growth policy function between a high-volatility state and a low-volatility state as a function of TFP, holding all other state variables fixed at their ergodic means.

Figure 9: Average and Standard Deviation of Growth Rate g for Different Interest Rate Scenarios

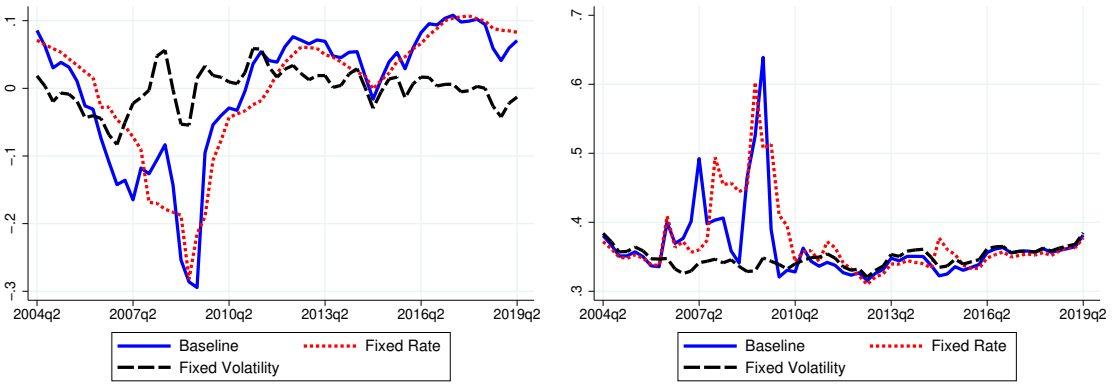

(a) Growth Rate g – Average

(b) Growth Rate g – Standard Deviation

Notes: This figure reports, for the baseline (Mexico) calibration, the cross-sectional average and standard deviation of the trend growth rate g under three scenarios: (i) full model with stochastic interest rates and volatility, (ii) interest rate volatility fixed at its mean, and (iii) interest rate level fixed at its mean while volatility follows its stochastic process. Panel (a) shows the cross-sectional average; panel (b) shows the cross-sectional standard deviation. All constructions mirror those in Figure 8.

Two observations are key. First, for productivity levels close to or above the ergodic mean, the effect of volatility on trend growth is similar across the three economies: the gap between high and low volatility is stable and modest. Second, once productivity is sufficiently low for the baseline (emerging-market) calibration to enter the constrained region, the relationship changes sharply. The gap in trend growth across volatility regimes steepens rapidly as productivity declines, reflecting Fisherian amplification when the constraint binds. Consequently, economies that fall into low-productivity states experience a much larger drop in trend growth in high-volatility states than economies that remain outside the constrained region, generating substantial cross-sectional dispersion even though the global volatility cycle is common.

A complementary way to quantify how often the economy is exposed to this nonlinear amplification is to measure how frequently the collateral constraint binds in normal times. In a simulation that fixes (R, σ_R) at their ergodic means and feeds the economy only idiosyncratic TFP shocks (with debt and other endogenous states adjusting), the borrowing constraint binds 7.1% of the time in the baseline calibration. This provides a benchmark for the stationary probability of operating in the nonlinear region. During high-volatility episodes, the set of states in which the constraint binds expands and the mass of constrained observations rises, magnifying dispersion. In contrast, within the constrained region the relaxed-constraint and advanced calibrations are less

sensitive to volatility increases because higher collateral pledgeability weakens the Fisherian feedback. This is also why the high–low volatility gap does not steepen—and can even *flatten*—in those calibrations: when financing is less tight, the labor-intensive component of innovation becomes relatively cheaper in bad times (wages fall), so R&D is less compressed (and can become partially countercyclical), offsetting the direct tightening effect of higher volatility. As a result, identical TFP shocks translate into much smaller differences in trend growth across economies and cross-sectional dispersion remains limited. The comparison between the baseline and relaxed-constraint calibrations highlights the role of pledgeability: it governs how frequently the economy enters the region where volatility has large marginal effects through collateral feedback.

Figure 10: Differential Effects of Volatility on Trend Growth

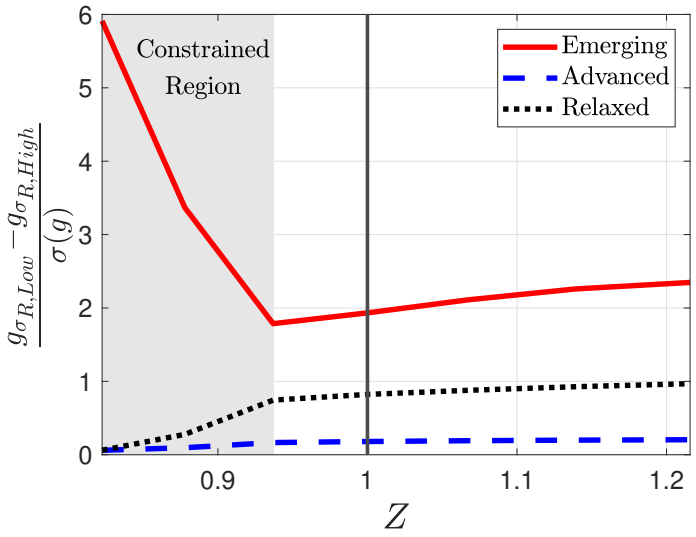

Notes: This figure plots, for each calibration, the difference in the policy function for the endogenous trend growth rate g between a high-volatility state and a low-volatility state, as a function of TFP. All other state variables are fixed at their ergodic means (including bond holdings and the interest rate). The shaded area denotes the set of TFP values for which the borrowing constraint binds in the baseline calibration when evaluated at ergodic-mean values of the other state variables. The vertical line indicates the ergodic mean of TFP. Trend-growth differences are standardized by the long-run standard deviation of g.

5 Conclusion

This paper provides empirical and theoretical evidence linking global financial risk to productivity trends, with particularly large effects in emerging markets. We operationalize global financial risk using uncertainty about U.S. interest rates. On the empirical side, we show that a one standard deviation increase in interest rate uncertainty lowers the level of the GDP trend in emerging

market economies by at least 25 basis points after three years, with substantially smaller effects in advanced economies. On the theoretical side, we develop a small open economy model with collateral constraints and endogenous innovation that can account for this heterogeneous response even when advanced and emerging economies are exposed to the same global shock process.

The model's mechanism operates through asymmetric responses and state dependence. Interest rate hikes sharply reduce trend productivity in emerging markets when collateral constraints bind, while cuts of equal magnitude produce only modest gains when constraints are slack. This asymmetry is amplified when financial risk is elevated. Higher rates compress firm values, tighten borrowing constraints through Fisherian deflation, trigger deleveraging, and reduce innovation and entry. Consequently, higher interest rate volatility lowers expected firm values and slows productivity growth even when average rates are unchanged.

In the model, heterogeneity arises from financial conditions rather than from differences in preferences, technology, or exogenous shocks. Advanced and emerging economies share identical primitives and face the same global processes, but differ in collateral tightness and spread levels. In the emerging market calibration, shutting down interest rate volatility substantially reduces trend-growth variation, while the advanced economy calibration is comparatively insensitive. The decomposition highlights that collateral constraints are the central source of amplification, with volatility sensitive risk premia accounting for the remainder.

Historical simulations illustrate the macroeconomic significance of the mechanism. During low-volatility periods, emerging markets accumulate productivity gains, whereas episodes of elevated global risk generate large and persistent reversals in trend productivity in the emerging market calibration while leaving the advanced economy calibration relatively stable. The model also reproduces higher cross-sectional dispersion of emerging market growth during high-risk periods despite identical global shocks.

These results imply that financial development shapes whether global financial instability remains a short-run cyclical disturbance or translates into persistent damage to productivity and long-run prosperity. Policies that raise effective pledgeability, through stronger contract enforcement and collateral recovery, deeper financial markets, and improved institutional frameworks, reduce the frequency and severity of binding constraint episodes and thereby attenuate the long run consequences of global risk shocks. Finally, because our empirical proxy focuses on uncer-

tainty about U.S. rates, it need not capture all episodes of emerging market stress driven by other sources of global or regional risk; incorporating broader measures of global risk is a natural direction for future work.

References

Adjemian, S., Bastani, H., Juillard, M., Mihoubi, F., Perendia, G., Ratto, M., and Villemot, S. (2011). 'Dynare: Reference manual, version 4'.

Aguiar, M. and Gopinath, G. (2007). 'Emerging market business cycles: The cycle is the trend'. *Journal of Political Economy*, vol. 115, no. 1, 69–102.

Akcigit, U. and Kerr, W. R. (2018). 'Growth through heterogeneous innovations'. *Journal of Political Economy*, vol. 126, no. 4, 1374–1443.

Akıncı, Ö. (2013). 'Global financial conditions, country spreads and macroeconomic fluctuations in emerging countries'. *Journal of International Economics*, vol. 91, no. 2, 358–371.

Akinci, O., Kalemli-Özcan, and Queralto, A. (2022). 'Uncertainty shocks, capital flows, and international risk spillovers'. Technical report, National Bureau of Economic Research.

Arellano, C. and Ramanarayanan, A. (2012). 'Default and the Maturity Structure in Sovereign Bonds'. *Journal of Political Economy*, vol. 120, no. 2, 187–232.

Ates, S. T. and Saffie, F. E. (2021). 'Fewer but better: Sudden stops, firm entry, and financial selection'. *American Economic Journal: Macroeconomics*, vol. 13, no. 3, 304–356.

Barnichon, R. and Matthes, C. (2018). 'Functional approximation of impulse responses'. *Journal of Monetary Economics*, vol. 99, 41–55.

Benguria, F., Matsumoto, H., and Saffie, F. (2022). 'Productivity and trade dynamics in sudden stops'. *Journal of International Economics*, vol. 139, 103631.

Benigno, G., Fornaro, L., and Wolf, M. (2025). 'The global financial resource curse'. *American Economic Review*, vol. 115, no. 1, 220–262.

Bhattarai, S., Chatterjee, A., and Park, W. Y. (2020). 'Global spillover effects of US uncertainty'. *Journal of Monetary Economics*, vol. 114, 71–89.

Bianchi, F., Ilut, C. L., and Schneider, M. (2018a). 'Uncertainty shocks, asset supply and pricing over the business cycle'. *The Review of Economic Studies*, vol. 85, no. 2, 810–854.

Bianchi, J. (2011). 'Overborrowing and Systemic Externalities in the Business Cycle'. *American Economic Review*, vol. 101, no. 7, 3400–3426.

Bianchi, J., Hatchondo, J., and Martinez, L. (2018b). 'International Reserves and Rollover Risk'. *American Economic Review*, vol. 108, no. 9, 2629–70.

Bianchi, J., Liu, C., and Mendoza, E. (2016). 'Fundamentals News, Global Liquidity and Macroprudential Policy'. *Journal of International Economics*, vol. 99, no. 1, 2–15.

Bianchi, J. and Mendoza, E. (2018). 'Optimal Time-consistent Macroprudential Policy'. *Journal of Political Economy*, vol. 6126, no. 2, 588–634.

Bianchi, J. and Mendoza, E. (2020). 'A Fisherian Approach to Financial Crises: Lessons from the Sudden Stops Literature'. *Review of Economic Dynamics*, vol. 37, S254–S283.

Bocola, L. and Gornemann, N. (2013). 'Risk, economic growth and the value of US corporations'.

Boz, E., Daude, C., and Durdu, C. B. (2011). 'Emerging market business cycles: Learning about the trend'. *Journal of Monetary Economics*, vol. 58, no. 6-8, 616–631.

Carrière-Swallow, Y. and Céspedes, L. F. (2013). 'The impact of uncertainty shocks in emerging economies'. *Journal of International Economics*, vol. 90, no. 2, 316–325.

Cerra, V. and Saxena, S. C. (2008). 'Growth dynamics: the myth of economic recovery'. *American Economic Review*, vol. 98, no. 1, 439–57.

Chang, R. and Fernández, A. (2013). 'On the sources of aggregate fluctuations in emerging economies'. *International Economic Review*, vol. 54, no. 4, 1265–1293.

Chari, A., Dilts-Stedman, K., and Forbes, K. (2022). 'Spillovers at the extremes: The macroprudential stance and vulnerability to the global financial cycle'. *Journal of International Economics*, vol. 136, 103582.

Comin, D. and Gertler, M. (2006). 'Medium-term business cycles'. *American Economic Review*, vol. 96, no. 3, 523–551.

Drechsel, T. (2023). 'Earnings-based borrowing constraints and macroeconomic fluctuations'. *American Economic Journal: Macroeconomics*, vol. 15, no. 2, 1–34.

Fernández-Villaverde, J., Guerrón-Quintana, P., Rubio-Ramirez, J. F., and Uribe, M. (2011). 'Risk matters: The real effects of volatility shocks'. *American Economic Review*, vol. 101, no. 6, 2530–61.

Garcia-Cicco, J., Pancrazi, R., and Uribe, M. (2010). 'Real business cycles in emerging countries?' *American Economic Review*, vol. 100, no. 5, 2510–31.

Garga, V. and Singh, S. R. (2021). 'Output hysteresis and optimal monetary policy'. *Journal of Monetary Economics*, vol. 117, 871–886.

Gerding, F., Henriksen, E., and Simonovska, I. (2014). 'The risky capital of emerging markets'.

Gertler, M. and Karadi, P. (2011). 'A model of unconventional monetary policy'. *Journal of monetary Economics*, vol. 58, no. 1, 17–34.

Gertler, M. and Kiyotaki, N. (2015). 'Banking, liquidity, and bank runs in an infinite horizon economy'. *American Economic Review*, vol. 105, no. 7, 2011–2043.

Gilchrist, S. and Zakrajšek, E. (2012). 'Credit spreads and business cycle fluctuations'. *American economic review*, vol. 102, no. 4, 1692–1720.

Gornemann, N., Guerrón Quintana, P. A., and Saffie, F. (2025). 'Real Exchange Rates and Endogenous Productivity'. *American Economic Journal: Macroeconomics*, vol. 17, no. 4, 204–261.

Gruss, B. and Mertens, K. (2009). 'Regime switching interest rates and fluctuations in emerging markets'.

Guerron-Quintana, P. A. and Jinnai, R. (2019). 'Financial frictions, trends, and the great recession'. *Quantitative Economics*, vol. 10, no. 2, 735–773.

Hegarty, C., Moretti, M., Ottonello, P., and Perez, D. (2023). 'Global Borrowing Costs and Firms' Risk in Open Economies'. *Working Paper*.

Husted, L., Rogers, J., and Sun, B. (2020). 'Monetary policy uncertainty'. *Journal of Monetary Economics*, vol. 115, 20–36.

INEGI and CONACYT (2019). 'INEGI y CONACYT presentan resultados de la Encuesta sobre Investigación y Desarrollo Tecnológico (ESIDET) 2017'. *INEGI Statistical Bulletin*, , no. 633/19.

Instituto Nacional de Estadística y Geografía (INEGI) (2021). 'El INEGI presenta los resultados del Estudio sobre la Demografía de los Negocios 2021'. Comunicado de prensa Núm. 790/21. 21 de diciembre de 2021.

Jarociński, M. and Karadi, P. (2020). 'Deconstructing monetary policy surprises—the role of information shocks'. *American Economic Journal: Macroeconomics*, vol. 12, no. 2, 1–43.

Johri, A., Khan, S., and Sosa-Padilla, C. (2022). 'Interest Rate Uncertainty and Sovereign Default Risk'. *Journal of International Economics*, vol. 139.

Jordà, Ò., Singh, S. R., and Taylor, A. M. (2024). 'The long-run effects of monetary policy'. *Review of Economics and Statistics*, pages 1–49.

Jurado, K., Ludvigson, S. C., and Ng, S. (2015). 'Measuring uncertainty'. *American Economic Review*, vol. 105, no. 3, 1177–1216.

Klette, T. J. and Kortum, S. (2004). 'Innovating Firms and Aggregate Innovation'. *Journal of Political Economy*, vol. 112, no. 5, 986–1018.

Koop, G., Pesaran, M. H., and Potter, S. M. (1996). 'Impulse response analysis in nonlinear multivariate models'. *Journal of econometrics*, vol. 74, no. 1, 119–147.

Lakdawala, A., Moreland, T., and Schaffer, M. (2021). 'The international spillover effects of US monetary policy uncertainty'. *Journal of International Economics*, vol. 133, 103525.

Lane, P. and Milesi-Ferretti, G. (2017). 'International Financial Integration in the Aftermath of the Global Financial Crisis'. *IMF Working Paper 17/115*.

Lian, C. and Ma, Y. (2021). 'Anatomy of corporate borrowing constraints'. *The Quarterly Journal of Economics*, vol. 136, no. 1, 229–291.

Mendoza, E. (2005). 'Real Exchange Volatility and the Price of Nontradables in Sudden-Stop Prone Economies'. *Economia*, pages 103–148. Fall.

Mendoza, E. G. (1991). 'Real business cycles in a small open economy'. *The American Economic Review*, pages 797–818.

Mendoza, E. G. (2010). 'Sudden stops, financial crises, and leverage'. *American Economic Review*, vol. 100, no. 5, 1941–66.

Miranda-Agrippino, S. and Rey, H. (2020). 'US monetary policy and the global financial cycle'. *The Review of Economic Studies*, vol. 87, no. 6, 2754–2776.

Moran, P. and Queralto, A. (2018). 'Innovation, productivity, and monetary policy'. *Journal of Monetary Economics*, vol. 93, 24–41.

Moris, F. and Shackelford, B. (2020). 'Labor Costs Account for Over Two-Thirds of U.S. Business RD Performance in 2020'. *National Center for Science and Engineering Statistics (NCSES)*, vol. 23.

Neumeyer, P. A. and Perri, F. (2005). 'Business cycles in emerging economies: the role of interest rates'. *Journal of monetary Economics*, vol. 52, no. 2, 345–380.

Queralto, A. (2020). 'A model of slow recoveries from financial crises'. *Journal of Monetary Economics*, vol. 114, 1–25.

Rey, H. (2015). 'Dilemma not trilemma: the global financial cycle and monetary policy independence'. Technical report, National Bureau of Economic Research.

Reyes-Heroles, R. and Tenorio, G. (2020). 'Macroprudential policy in the presence of external risks'. *Journal of International Economics*, vol. 126, 103365.

Roch, F., Urquiza, J., and Vicondoa, A. (2025). 'Spillovers of US Policy Volatility Shocks to EMEs'. *Mimeo*.

Tauchen, G. (1986). 'Finite State Markov-Chain Approximations to Univariate and Vector Autoregressions'. *Economics Letters*, vol. 20, no. 2, 177–181.

Uribe, M. and Yue, V. Z. (2006). 'Country spreads and emerging countries: Who drives whom?' *Journal of international Economics*, vol. 69, no. 1, 6–36.

Valdivia López, M. and Borrayo López, R. (2023). 'Una estimación de los activos intangibles para la economía mexicana: 1990-2020'. *Problemas del Desarrollo*, vol. 54, no. 215, 55–87.

Vicondoa, A. (2019). 'Monetary news in the United States and business cycles in emerging economies'. *Journal of International Economics*, vol. 117, 79–90.

World Bank (2020). 'Doing Business 2020: Comparing Business Regulation in 190 Economies'. *World Bank Report*.

Zhou, H. (2024). 'The fickle and the stable: Global financial cycle transmission via heterogeneous investors'. *Available at SSRN 4616182*.

Appendices

Appendix A Empirical Appendix

In this section we provide additional details on the data construction and empirical methods underlying the results in Section 2. We describe how we measure U.S. interest rate uncertainty, outline the estimation of stochastic volatility in real interest rates, and report supporting evidence and robustness checks that validate our empirical implementation.

A.1 Data and Stochastic Volatility in U.S. Real Rates

For the United States, we utilize data on PCE inflation and Treasury interest rates (3-month, 2-year, 5-year) from FRED. We construct a demeaned quarterly time series for the U.S. real interest rate, measured as the real 3-month T-bill rate, for the period of interest.[32] Following Fernández-Villaverde et al. (2011), we adjust nominal rates by the total change in the PCE index over the current and prior three quarters. We estimate the stochastic volatility of the U.S. real interest rate using the particle filter methodology described by Fernández-Villaverde et al. (2011). Specifically, we filter a sequence σ_t from the following model, estimated by maximum likelihood:

$$R_t - \bar{R} = \phi(R_{t-1} - \bar{R}) + \sigma_t^r \varepsilon_t^r, \tag{29}$$

$$\log \sigma_t^r = (1 - \rho_\sigma^r)\mu_\sigma^r + \rho_\sigma^r \log \sigma_{t-1}^r + \sigma_r \nu_t^r, \tag{30}$$

where $\bar{R}$ represents the sample mean of the real interest rate.

Table 5 presents our parameter estimates. Both the interest rate and its hidden volatility state are highly persistent. Figure 11 displays the real interest rate and the smoothed path of the volatility state. Notably, the hidden volatility state shows substantial variation over time. Volatility declines from 1985 to 2000, corresponding to the relative stability in real rates during this period. Afterward, volatility rises over the next decade, paralleling a persistent decline in the average rate and significant fluctuations around this trend. Post-2010, real rates stabilize again, which is reflected in the stochastic volatility process.

[32] Using the 2-year or 5-year interest rate instead does not significantly alter our core findings, as these series are highly correlated over the sample period.

Table 5: U.S. Interest Rate Model: Estimated Parameters

ϕ	ρ_σ^r	μ_σ^r	σ_r
0.9115	0.9387	−6.3516	0.1181
(0.88,0.93)	(0.88,0.95)	(−6.61,−6.09)	(0.02,0.20)

Notes: This table reports maximum likelihood estimates for the stochastic volatility model of the U.S. real interest rate described in equations (29)–(30). Parentheses contain 95% confidence intervals obtained via monte carlo simulations.

Figure 11: Estimated Series for U.S. Real Rates

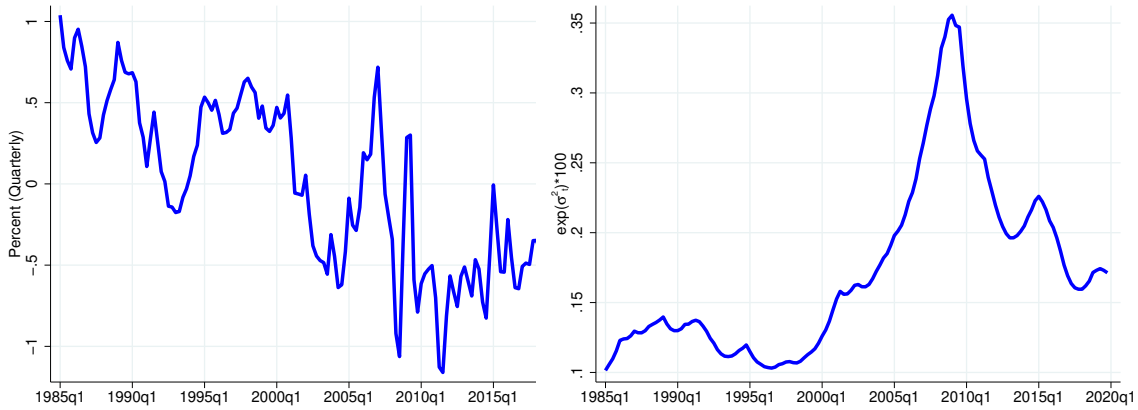

(a) U.S. Real Interest Rate

(b) U.S. Real Interest Rate Stochastic Volatility

Notes: Panel (a) plots the demeaned quarterly U.S. real 3-month T-bill rate. Panel (b) shows the smoothed stochastic volatility state implied by the model in equations (29)–(30).

A.2 Time Series Models

Here we gather more details on the estimated time series models.

Our baseline specification is:

$$\begin{pmatrix} \Delta y_{j,t} \\ \Delta c_{j,t} \\ \Delta i_{j,t} \end{pmatrix} = \begin{pmatrix} \alpha_j \\ \alpha_j \\ \alpha_j \end{pmatrix} + A \cdot \left(\begin{pmatrix} \Delta y_{j,t-1} \\ \Delta c_{j,t-1} \\ \Delta i_{j,t-1} \end{pmatrix} - \begin{pmatrix} 1 \\ 1 \\ 1 \end{pmatrix} \hat{a}_{j,t-1} \right) + \begin{pmatrix} 1 \\ 1 \\ 1 \end{pmatrix} \hat{a}_{j,t} + B \cdot Z_t^{US} + \Sigma_j \epsilon_{j,t}^m$$

$$\begin{aligned} \hat{a}_{j,t} &= a_{j,t} + \left(\sum_{s=0}^{n_\sigma} \eta_s \sigma_{t-s}^{MU} \right) \\ a_{j,t} &= \rho_a a_{j,t-1} + \sigma_{j,a} \epsilon_{j,t}^a. \end{aligned}$$

For most of our results we also impose $\eta_s = a \cdot \exp\left(-\frac{s-b}{c}\right)$. When we estimate the model, we impose that $\rho_a \in (-1, 1)$ and that Σ_j is diagonal. We assume that all innovations are drawn from a joint normal distribution and that shocks to the trend $(\epsilon^a_{j,t})$ are independent from $\epsilon^m_{j,t}$. To reduce the number of parameters to estimate in our baseline results we also set

$$B \cdot Z^{US}_t = B_1 \cdot (\Delta Y^{US}_t, \Delta Y^{US}_{t-1}, EBP_t, EBP_{t-1}) + \begin{pmatrix} b^y_2 \\ b^c_2 \\ b^i_2 \end{pmatrix} \left(\sum_{s=0}^{n^s_\sigma} \eta^v_s \Delta \sigma^{MU}_{t-s} \right)$$

and impose the same parametric form as discussed above on the η^b_s. So, while we leave the response to U.S. growth (ΔY^{US}_t) and the excess bond premium (EBP_t) unrestricted we impose some restrictions on the transitory effects of the uncertainty shock. Relaxing the latter by allowing B to be fully unrestricted leads to similar point estimates for the η_s but wider error bands.

To compute standard errors we repeat the estimation on model simulated data 1000 times and compute the percentiles of interest. In order to simulate the U.S. variables in this process, we fit a VAR(2) to the U.S. time series.

In addition to using different time series proxies for uncertainty we also performed various variations of the main specification to assess robustness and found our main result survives. As already noted we allowed for different restrictions on B. We also dropped some or all of the U.S. controls. We estimated the model both with and without the parametric restrictions on the η_s.

Finally, we separated the effect of the U.S. variables on the trend from other, transitory effects, by estimating:

$$\begin{pmatrix} \Delta y_{j,t} \\ \Delta c_{j,t} \\ \Delta i_{j,t} \end{pmatrix} = \begin{pmatrix} \alpha_j \\ \alpha_j \\ \alpha_j \end{pmatrix} + A \cdot \left(\begin{pmatrix} \Delta y_{j,t-1} \\ \Delta c_{j,t-1} \\ \Delta i_{j,t-1} \end{pmatrix} - \begin{pmatrix} 1 \\ 1 \\ 1 \end{pmatrix} \hat{a}_{j,t-1} \right) + \begin{pmatrix} 1 \\ 1 \\ 1 \end{pmatrix} \hat{a}_{j,t} + \tilde{B} \cdot \tilde{Z}^{US}_t + \Sigma_j \epsilon^m_{j,t}$$

$$\begin{aligned}\hat{a}_{j,t} &= a_{j,t} + \left(\sum_{s=0}^{n_\sigma} \eta_s \sigma_{t-s}^{MU}\right) + C \cdot (\Delta Y_t^{US}, EBP_t) \\ a_{j,t} &= \rho_a a_{j,t-1} + \sigma_{j,a} \epsilon_{j,t}^a.\end{aligned}$$

Here

$$\begin{aligned}\tilde{B} \cdot Z_t^{US} &= \tilde{B}_1 \cdot (\Delta Y_t^{US} - \Delta Y_{t-1}^{US}, \Delta Y_{t-1}^{US} - \Delta Y_{t-2}^{US}, EBP_t - EBP_{t-1}, EBP_{t-1} - EBP_{t-2}) \\ &+ \begin{pmatrix} b_2^y \\ b_2^c \\ b_2^i \end{pmatrix} \left(\sum_{s=0}^{n_\sigma^s} \eta_s^v \Delta \sigma_{t-s}^{MU}\right).\end{aligned}$$

In this way we impose a separation between permanent and transitory effects of U.S. variables. Results on the η_s are again robust. We use the smoothed estimate for $a_{j,t} + \left(\sum_{s=0}^{n_\sigma} \eta_s \sigma_{t-s}^{MU}\right) + C \cdot (\Delta Y_t^{US}, EBP_t)$ as our estimate of the country trend whenever we display them in the main text to allow more explicitly for other U.S. effects on the trend.

Figure 12 shows the confidence intervals when we replace the monetary policy uncertainty shocks with shocks based on other uncertainty metrics as discussed in the text. All of them are identified as the residuals from a VAR including U.S. GDP growth, CPI inflation, interest rates, and the excess bond premium. Figure 13 replaces the uncertainty measure with U.S. monetary policy shocks as measured by Jarociński and Karadi (2020) using the median-rotation. The shock is scaled so that it moves U.S. 2-year rates by 25 basis points.

Figure 12: Trend Response to Uncertainty Shocks, Robustness: Confidence Intervals

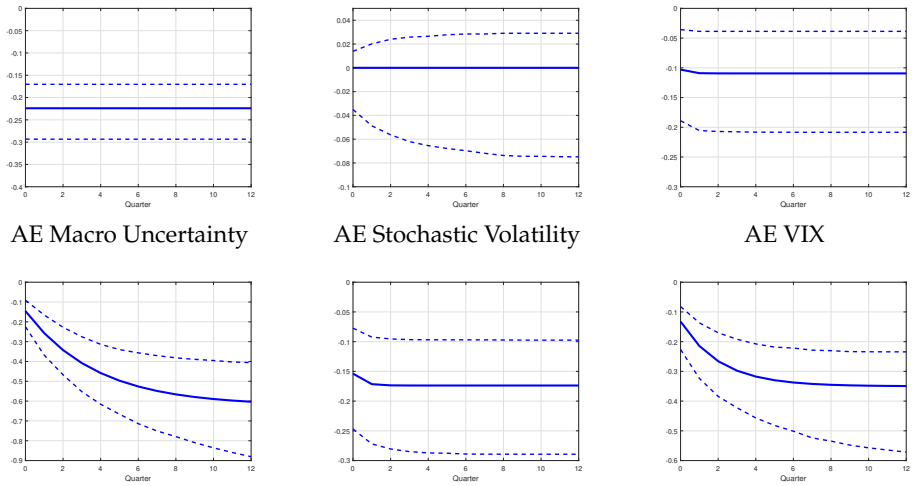

Notes: This figure plots the cumulative response of the estimated stochastic trend to a one-standard-deviation global uncertainty shock for advanced economies (top) and emerging economies (bottom). The lines report responses when the uncertainty shock is proxied by (i) macroeconomic uncertainty from Jurado et al. (2015), (ii) the stochastic volatility of the U.S. real short rate following Fernández-Villaverde et al. (2011), (iii) the VIX index. All responses are estimated under the parametric restriction on η_s and include the same set of U.S. controls as in the baseline specification. Solid lines show the point estimate, while the broken lines indicate 1-std error bands.

Figure 13: Trend Response to U.S. Monetary Policy Shock

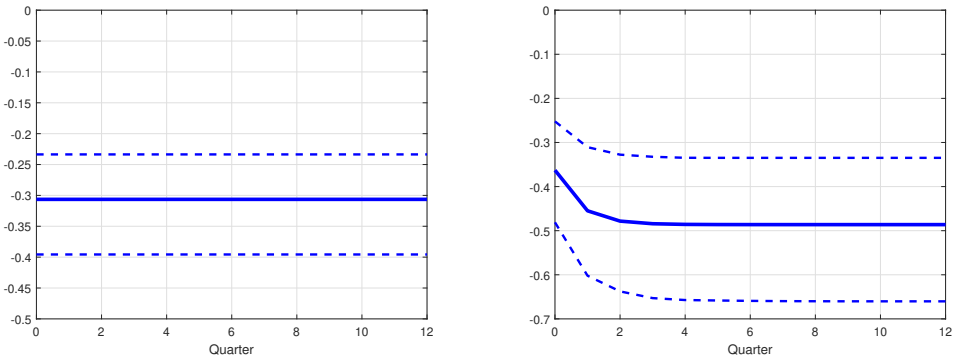

Notes: This figure plots the cumulative response of the estimated stochastic trend to a one-standard-deviation monetary policy shock for advanced economies (left) and emerging economies (right). Solid lines show the point estimate, while the broken lines indicate 1-std error bands. We use the median-rotation U.S. monetary policy shocks from Jarociński and Karadi (2020) and scale responses so that the shocks move the annualzied U.S. 2-year rate by 25 basis points.

Appendix B A Simple Model with a Financial Accelerator

In this appendix, we characterize a simple model following Gertler and Karadi (2011), Gertler and Kiyotaki (2015), and Akinci et al. (2022), where financial intermediaries in the economy face stochastic volatility in deposit rates. The rest of the features of the model are standard in this literature.

B.1 Model Setup

The optimization problem of an individual bank is

$$\begin{aligned} V_{i,t} &= \max_{L_{i,t}, D_{i,t}} \mathbb{E}_t \left[\Lambda_{t,t+1} \left((1-\sigma) N_{i,t+1} + \sigma V_{i,t+1} \right) \right] \\ \text{subject to} \quad & V_{i,t} \geq \theta L_{i,t} \\ & N_{i,t} = R^l_{t-1} L_{i,t-1} - R^d_{t-1} D_{i,t-1} \\ & N_{i,t} + D_{i,t} = L_{i,t} \end{aligned}$$

We assume that the loan demand is given by $L(R^l_t) = A - B \cdot R^l_t$. The bond interest rate follows the stochastic process:

$$\begin{aligned} R^d_t &= R^d + \rho_1 (R^d_{t-1} - R^d) + \sigma_{t-1} \epsilon_t \\ \log \sigma_t &= \log \bar{\sigma} + \rho_2 (\log \sigma_{t-1} - \log \bar{\sigma}) + \bar{\sigma} \eta_t. \end{aligned}$$

Lastly, $\Lambda_{t,t+1}$ is the relevant discount factor and $\Lambda_{t,t+1} = \frac{1}{R^d_t}$.

B.2 Quantitative Results

We calibrate the model to match features of the U.S. economy. Table 6 presents the externally calibrated parameters, along with their corresponding values and sources in the data. The parameters for the stochastic process of the real interest rate and volatility are the ones presented in Section A.1.

Table 6: Calibration Summary

Parameter	Symbol	Value	Source
Deposit Rate	R^d	1.005	U.S. data
Demand Parameters	A, B	Internal	Normalization $L = 1$
Exit Probability	$1 - \sigma$	0.03	U.S. data
Leverage Ratio	L/N	5	U.S. data
Loan Rate	R^l	1.0075	U.S. data

Notes: This table reports the externally calibrated parameters for the banking model in Appendix B. The deposit rate, leverage ratio, exit probability, and average loan rate are chosen to match U.S. bank-level and aggregate data. The demand parameters A and B are internally set to normalize steady-state lending to $L = 1$. The stochastic processes for interest rates and volatility follow the estimates in Section A.1.

The rest of the parameters, Ω, ψ, ν, and θ, are set internally such that equilibrium conditions are satisfied. Figure 14 presents the impulse response functions of the model in response to a one standard deviation increase in interest rate volatility.[33] Responses appear as percentage point deviations from their corresponding steady state values. We also add the responses of an alternative calibration (black dotted line). This calibration assumes that the average loan-deposit rate spread is higher than in the baseline scenario ($R^L = 1.0085$). This assumption is consistent with an economy that features a larger value of the parameter ι, which controls the average spread faced by agents in the economy.

Figure 14: Impulse Response Functions to a Stochastic Volatility Shock

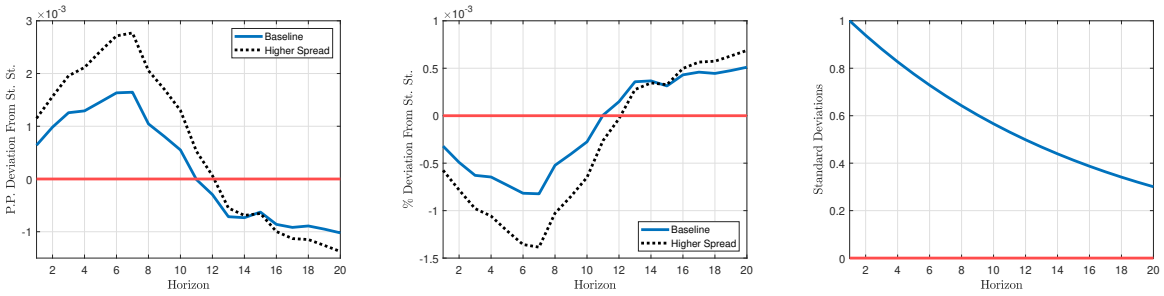

Loan Interest Rate R^l | Loans L_t | Stochastic Volatility σ_t

Notes: This figure shows impulse responses to a one standard deviation increase in the volatility of the deposit rate. Solid lines correspond to the baseline calibration, while dotted lines depict an alternative calibration with a higher average loan–deposit spread. Panel (a) shows the loan rate R^l, panel (b) the quantity of loans L_t, and panel (c) the volatility state σ_t.

[33] We solve this model using 3rd order perturbation in dynare. As the impulse response functions are obtained as the average over the ergodic set through simulation some noise remains in the figures. For more on dynare see Adjemian et al. (2011).

The impulse response functions of the baseline case presented in Figure 14 show that an increase in interest rate volatility leads to an increase in the borrowing costs faced by agents in the economy, which ultimately leads to a decrease in borrowing. Interestingly, the exercise also shows that an economy that has a larger average loan-deposit spread is also more sensitive to a volatility shock: loan rate increases and lending declines are more pronounced relative to the baseline.

Appendix C Financial Intermediation, Risk Aversion and Volatility

As seen in Equation (7), a change in the volatility state has a level effect on the interest rate, in addition to altering the dispersion of interest rate innovations. To separate these effects, we build a counterfactual in which the only shock corresponds to the level effect coming from ι_1 in Equation (7). In this setup, the only impact is a direct effect on the price of debt, fully isomorphic to a first-moment shock in interest rates. By comparing the impulse response to this shock with the baseline response to a volatility shock, we can decompose the effect into first- and second-moment components. Furthermore, we replicate this exercise for the three calibrations examined in the main text (baseline, advanced, and relaxed constraint economies).[34]

To generate the isomorphic interest rate, we proceed as follows. We begin by generating a cross-section of stochastic volatility shocks, as used in Section 4.2. For each of these sequences, we compute the implied interest rate that would produce the same observed movement in the price $\hat{q}(s^t)$. We then compute impulse responses to this implied interest rate shock. The first panel of Figure 15 presents the cumulative trend responses to the full stochastic volatility shock and to the implied interest rate shock for the baseline model. The second panel shows the difference in responses between the baseline and the two counterfactual models, where in each case we calculate the model-specific implied R sequence. Because the second panel nets out the level effect, these differences can be interpreted as the pure second-moment effect on interest rates.

[34] See Section 4 for more details about the calibration and the economies studied.

Figure 15: Cumulative Trend Responses, Stochastic Volatility and Interest Rate Shocks

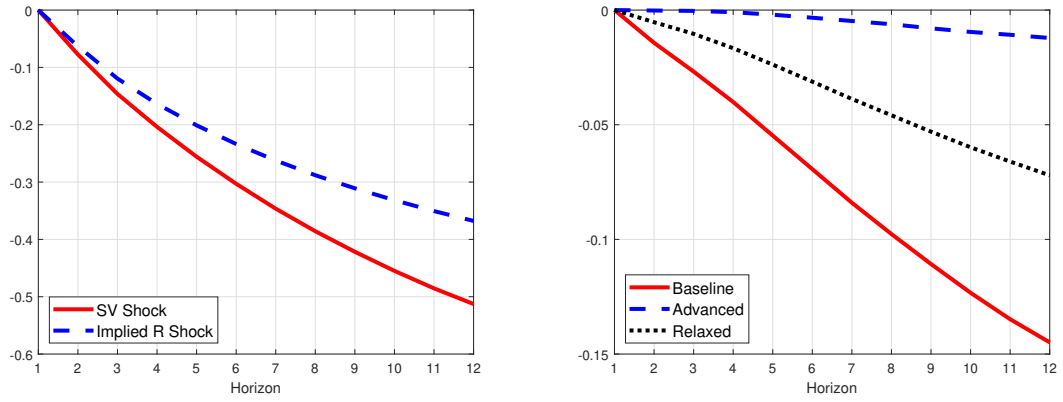

(a) Cumulative Responses (b) Differential Responses (SV − Implied R)

Notes: Panel (a) presents the cumulative trend responses to a one standard deviation volatility shock and to the implied first-moment interest rate shock for the baseline calibration. Panel (b) shows the difference between the cumulative responses to the stochastic volatility shock and the implied rate shock, for the baseline, advanced, and relaxed constraint economies. These differences isolate the pure second-moment (volatility) effect on trend productivity.

The results in the first panel of Figure 15 show that pure volatility explains roughly 30% of the total response to a volatility shock. While the level effect varies across models with different ι_1, the pure second-moment effect can only differ due to the internal propagation mechanisms within each model. The second panel of Figure 15 confirms that the collateral constraint plays a key role in this propagation. Interestingly, there remains an important difference between the advanced and relaxed economies, which differ only in their average spread and in the first-moment channel of stochastic volatility. This difference arises from the fact that the relaxed economy features a different ergodic distribution and a distinct frequency and severity of Sudden Stops. Thus, more volatile rates can still trigger relatively asymmetric effects through the interaction of the two channels.

Appendix D Calculating the Firm Size Distribution

Because there is a continuum of products we can use the law of large numbers to track the distribution of firms. In particular, denote by $\Omega_n(s^t)$ the mass of firms with n products. The law of motion of this distribution is characterized by a system of dynamic equations that only depend on

the innovation rate of incumbents and the mass of entrants:

$$\begin{aligned}
\Omega_1(s^t) &= \left(M^*(s^{t-1})\right)^{\upsilon} + \sum_{n=1}^{\infty}\Omega_n(s^{t-1})\sum_{k=0}^{1}\mathbb{B}\left(k,n,x^*(s^{t-1})\right)\mathbb{B}\left((k+n-1,n,\Delta(s^{t-1})\right)\\
\Omega_{\tilde{n}>1}(s^t) &= \sum_{n=\mathbb{I}^+(\frac{\tilde{n}}{2})}^{\tilde{n}}\left\{\Omega_n(s^{t-1})\sum_{k=\tilde{n}-n}^{n}\mathbb{B}\left(k,n,x^*(s^{t-1})\right)\mathbb{B}\left(k-(\tilde{n}-n),n,\Delta(s^{t-1})\right)\right\}\\
&+ \sum_{n=\tilde{n}+1}^{\infty}\left\{\Omega_n(s^{t-1})\sum_{k=0}^{\tilde{n}}\mathbb{B}\left(k,n,x^*(s^{t-1})\right)\mathbb{B}\left(k-(\tilde{n}-n),n,\Delta(s^{t-1})\right)\right\},
\end{aligned}$$

where $\mathbb{I}^+(a)$ refers to the integer closest to a such that $\mathbb{I}^+(a) \geq a$.[35] The first equation has two terms, the first one tracks the entry of new firms with one product while the second term tracks firms that used to have more than 1 product and contracted to exactly 1 product. The second line shows an analogous law of motion for categories of firms with more than one product where the first component are firms that started with less than $\tilde{n}$ products and had net gains that left them at $\tilde{n}$, while the second term reflects firms that were above $\tilde{n}$ and experienced net losses that left them exactly at $\tilde{n}$.[36] The BGP distribution can be found by iterating in these laws of motion until the mass of firms in each product category is constant.

Appendix E Dynamic System of Equations

E.1 Representative Household & Financial Intermediation

$$\begin{aligned}
\tilde{m}(s^t,s_{t+1}) &= \beta\frac{\tilde{C}(s_{t+1})^{-\gamma}}{\tilde{C}(s^t)^{-\gamma}-\phi\tilde{\mu}(s^t)}(1+g(s^t,s_{t+1}))^{-\gamma}\\
\tilde{C}(s^t)^{-\gamma} &= \tilde{\mu}(s^t)+\frac{\beta}{\hat{q}(s^t)}\mathbb{E}\left[\tilde{C}(s^{t+1})^{-\gamma}|s^t\right](1+g(s^t,s_{t+1}))^{-\gamma}\\
\tilde{C}(s^t)+\hat{q}(s^t)\tilde{B}^H(s^t)(1+g(s^t,s_{t+1})) &= \tilde{w}(s^t)+\tilde{B}^H(s^{t-1})+\tilde{T}(s^t)\\
\hat{q}(s^t)\tilde{B}^H(s^t)(1+g(s^t,s_{t+1})) &\geq -\phi\Lambda\tilde{V}_1(s^t)\\
\hat{q}(s^t) &= \mathbb{E}\left[\frac{1}{(1+R(s^{t+1})+\iota_0+\iota_1(\sigma(s^{t+1})-\bar{\sigma}))}\middle|s^t\right].
\end{aligned}$$

[35] A firm with n products can become a firm with $n' \in [0, 2n]$ in one period, so at most it can double its size in one period.

[36] The condition that ensures that the mass of products is always equal to one is given by $\sum_{n=1}^{\infty} n\Omega_n(s^t) = \Lambda$.

E.2 Final Good Producer

$$\tilde{Y}(s^t) = e^{z(s^t)} l(s^t).$$

E.3 Intermediate Good Producer

$$\begin{aligned}
l(s^t) &= \frac{\tilde{Y}(s^t)}{\tilde{w}(s^t)\Lambda(1+\sigma)} \\
\tilde{\pi}(s^t) &= \frac{\sigma}{\Lambda(1+\sigma)}\tilde{Y}(s^t) \\
\tilde{V}_1(s^t) &= \tilde{\pi}(s^t) - \alpha\tilde{w}(s^t)\left(\frac{x(s^t)}{\xi}\right)^{\frac{1}{\theta}} - (1-\alpha)x(s^t)F + \\
&\quad \mathbb{E}\left[\tilde{m}(s^{t+1})(1-\Delta(s^t)+x(s^t))\left(1+g\left(s^t,s_{t+1}\right)\right)\tilde{V}_1(s^{t+1})|s^t\right] \\
x^*(s^t) &= \left[\frac{\theta}{\alpha}\xi^{\frac{1}{\theta}}\frac{\mathbb{E}\left[\tilde{m}(s^{t+1})\left(1+g\left(s^t,s_{t+1}\right)\right)\tilde{V}_1(s^{t+1})\middle|\, s_t\right]-(1-\alpha)F}{\tilde{w}(s^t)}\right]^{\frac{\theta}{1-\theta}} \\
l_r(s^t) &= \left(\frac{x(s^t)}{\xi}\right)^{\frac{1}{\theta}}.
\end{aligned}$$

E.4 Entry

$$M^*(s^t) = \left[\frac{v}{\alpha\kappa}\frac{\mathbb{E}\left[\tilde{m}(s^{t+1})\left(1+g\left(s^t,s_{t+1}\right)\right)\tilde{V}_1(s^{t+1})|s^t\right]-(1-\alpha)F}{\tilde{w}(s^t)}\right]^{\frac{1}{1-v}}.$$

E.5 Aggregate Variables

$$\begin{aligned}
1+g(s^t,s_{t+1}) &= (1+\sigma)^{\Delta}(1-\delta) = (1+\sigma)^{x^*(s^t)+\frac{(M^*(s^t))^v}{\Lambda}}(1-\delta) \\
\tilde{T}(s^t) &= \Lambda\left[\tilde{\pi}(s^t) - \tilde{w}(s^t)\alpha\left(\frac{x(s^t)}{\xi}\right)^{\frac{1}{\theta}} - (1-\alpha)x(s^t)F\right] - \kappa\alpha M^*(s^t)\tilde{w}(s^t) - (1-\alpha)\left(M^*(s^t)\right)^v F \\
\tilde{w}(s^t) &= \frac{e^{z(s^t)}}{\Lambda(1+\sigma)} \\
1 &= \Lambda\left(l(s^t)+l_r(s^t)\right) + \kappa M^*(s^t).
\end{aligned}$$

E.6 Exogenous Shocks

$$
\begin{aligned}
\ln z(s^t) &= \rho_z \ln z(s^{t-1}) + \epsilon_t, \quad \text{with} \quad \epsilon_t \sim N(0, \eta_z^2) \\
R(s^t) - \bar{R} &= \phi_R \left(R(s^{t-1}) - \bar{R} \right) + \sigma(s^t)\omega(s^t), \quad \text{with} \quad \omega(s^t) \sim N(0,1), \\
\log(\sigma(s^t)) &= (1-\rho_\sigma)\mu_\sigma + \rho_\sigma \log(\sigma(s^{t-1})) + \eta_\sigma \nu(s^t), \quad \text{with} \quad \nu(s^t) \sim N(0,1),
\end{aligned}
$$

Appendix F Solution Method

Our solution algorithm for the decentralized equilibrium follows a combination of the time-iteration method employed in Bianchi et al. (2016) with value function iteration. We extend it in order to update guesses for the continuation value of a product line.

We discretize the processes for aggregate efficiency z, interest rate R and volatility σ_r following Tauchen (1986). We consider grids of 7 points for aggregate efficiency, 21 points for the interest rate, and 9 points for interest rate volatility. Our bond holdings grid consists of 60 points, and is skewed towards larger debt holdings.[37]

In what follows we drop the superscript H from bond holdings B^H in order to save notation. All functions presented below are stationary, unless otherwise noted. We start with a conjecture for the bond holdings policy function, B', defined over the state space (z, R, σ_r, B).[38] We also make a guess for innovation intensity $x(z, R, \sigma_r, B)$. For notational simplicity, assume $\mathbf{S} = (z, R, \sigma_r)$.

The steps of the solution algorithm are the following:

1. Start iteration j with a guess for $B'_j(\mathbf{S}, B)$ and innovation intensity $x_j(\mathbf{S}, B)$. Using these guesses construct:

$$M_j(\mathbf{S}, B) = \left[\frac{x_j(\mathbf{S}, B)^{\frac{1-\theta}{\theta}}}{\xi^{\frac{1}{\theta}}\theta} \frac{\nu}{\kappa} \right]^{\frac{1}{1-\nu}} \tag{31}$$

$$g_j(\mathbf{S}, B) = (1+\sigma)^{x_j(\mathbf{S},B) + \frac{M_j(\mathbf{S},B)^\nu}{\Lambda}}(1-\delta) - 1 \tag{32}$$

$$\Delta_j(\mathbf{S}, B) = x_j(\mathbf{S}, B) + \frac{M_j(\mathbf{S}, B)^\nu}{\Lambda} \tag{33}$$

$$l_{rj}(\mathbf{S}, B) = \left(\frac{x_j(\mathbf{S}, B)}{\xi} \right)^{\frac{1}{\theta}} \tag{34}$$

$$l_j(\mathbf{S}, B) = \frac{(1 - \kappa M_j(\mathbf{S}, B))}{\Lambda} - l_{rj}(\mathbf{S}, B) \tag{35}$$

$$Y_j(\mathbf{S}, B) = z\, l_j(\mathbf{S}, B) \tag{36}$$

$$\pi_j(\mathbf{S}, B) = \frac{\sigma}{\Lambda(1+\sigma)} Y_j(\mathbf{S}, B) \tag{37}$$

[37] Since we interpolate policy functions, our results do not vary substantially with more populated grids.

[38] Note that this guess corresponds to a matrix with dimensions $N_z \times N_R \times N_\sigma \times N_B$, where N_z, N_R, N_σ and N_B correspond to the number of elements in the grid of aggregate efficiency, interest rate, volatility of interest rate and debt, respectively.

$$t_j(\mathbf{S}, B) = \Lambda(\pi_j(\mathbf{S}, B) - \alpha w(z) l_{rj}(\mathbf{S}, B) - (1-\alpha) F x_j(\mathbf{S}, B)) \\ - \alpha\kappa M_j(\mathbf{S}, B) w(z) - (1-\alpha) M_j(\mathbf{S}, B)^{\nu} F \tag{38}$$

$$w(\mathbf{S}) = \frac{\exp(z)}{\Lambda(1+\sigma)} \tag{39}$$

$$c_j(\mathbf{S}, B) = w(\mathbf{S}) + B - B'_j(\mathbf{S}, B)(1 + g_j(\mathbf{S}, B))\hat{q}(\mathbf{S}) + t_j(\mathbf{S}, B) \tag{40}$$

Lastly, compute the discounted expected marginal utility

$$\beta \frac{1}{\hat{q}(\mathbf{S})} \mathbb{E}\left[u_j(\mathbf{S}', B'_j(\mathbf{S}, B))\right] (1 + g_j(\mathbf{S}, B))^{-\gamma}, \tag{41}$$

where $u_j(\mathbf{S}, B) = c_j(\mathbf{S}, B)^{-\gamma}$.

2. Using the above guesses compute a guess for the value of a product line and the stochastic discount factor. For the value of a product line we iterate over the following value function:

$$V_{1,k+1}(\mathbf{S}, B) = \pi_j(\mathbf{S}, B) - \alpha w(\mathbf{S}) \left(\frac{x_j(\mathbf{S}, B)}{\xi}\right)^{\frac{1}{\theta}} - (1-\alpha) x_j(\mathbf{S}, B) F \\ + \mathbb{E}\left[m_j(\mathbf{S}, B)(1 - \Delta_j(\mathbf{S}, B) + x_j(\mathbf{S}, B))\left(1 + g_j(\mathbf{S}, B)\right) V_{1,k}(\mathbf{S}, B)\right] \tag{42}$$

until $||V_{1,k+1}(\mathbf{S}, B) - V_{1,k}(\mathbf{S}, B)|| < \text{tol}$. $V_{1,j}(\mathbf{S}, B)$ is the converged value function.

3. Assume the borrowing constraint binds. Note that when the constraint binds we have that consumption is

$$c_{j+1}(\mathbf{S}, B) = w(\mathbf{S}) + B + \phi\Lambda V_{1,j}(\mathbf{S}, B) + t_j(\mathbf{S}, B). \tag{43}$$

We then check whether this assumption holds by calculating the residual of the Euler equation:

$$\mathcal{R}(\mathbf{S}, B) = u_{j+1}(\mathbf{S}, B) \\ - \beta \frac{1}{\hat{q}(\mathbf{S})} \mathbb{E}\left[u_j(\mathbf{S}', B'_j(\mathbf{S}, B))\right] (1 + g_j(\mathbf{S}, B))^{-\gamma}. \tag{44}$$

If $\mathcal{R}(\mathbf{S}, B) > 0$, we keep the values for $c_{j+1}(\mathbf{S}, B)$, and we set $B'_{j+1}(\mathbf{S}, B) = -\frac{\phi \Lambda V_{1,j}(\mathbf{S},B)}{(1+g_j(\mathbf{S},B))\hat{q}(\mathbf{S})}$, $\mu_{j+1}(\mathbf{S}, B) = \mathcal{R}(\mathbf{S}, B)$. Otherwise, the constraint does not bind for that point of the state space and we discard $c_{j+1}(\mathbf{S}, B)$ and $B'_{j+1}(\mathbf{S}, B)$. We then numerically solve for the value of $c_{j+1}(\mathbf{S}, B)$ that satisfies

$$u_{j+1}(\mathbf{S}, B) = \beta \frac{1}{\hat{q}(\mathbf{S})} \mathbb{E}\left[u_j(\mathbf{S}', B'_j(\mathbf{S}, B))\right] (1 + g_j(\mathbf{S}, B))^{-\gamma}. \tag{45}$$

We then set $B'_{j+1}(\mathbf{S}, B) = \frac{w(\mathbf{S})+B+t_j(\mathbf{S},B)-c_{j+1}(\mathbf{S},B)}{(1+g_j(\mathbf{S},B))\hat{q}(\mathbf{S})}$ and $\mu_{j+1}(\mathbf{S}, B) = 0$.

4. Using the updated guesses $c_{j+1}(\mathbf{S}, B)$ and $B'_{j+1}(\mathbf{S}, B)$, compute an updated guess for the stochastic discount factor:

$$m_{j+1}(\mathbf{S}, B) = \beta \frac{c_{j+1}(\tilde{\mathbf{S}}', B'_{j+1}(\mathbf{S}, B))^{-\gamma}}{c_{j+1}(\mathbf{S}, B)^{-\gamma} - \phi \mu_{j+1}(\mathbf{S}, B)} (1 + g_j(\mathbf{S}, B))^{-\gamma}, \tag{46}$$

where $\tilde{\mathbf{S}}'$ are next-period realizations.

5. Recompute the value of a product line using the updated stochastic discount factor. That is, use value function iteration over the value of a product line:

$$\begin{aligned} V_{1,k+1}(\mathbf{S}, B) &= \pi_j(\mathbf{S}, B) - \alpha w(\mathbf{S}) \left(\frac{x_j(\mathbf{S}, B)}{\xi}\right)^{\frac{1}{\theta}} - (1 - \alpha) x_j(\mathbf{S}, B) F \\ &+ \mathbb{E}\left[m_{j+1}(\mathbf{S}, B)(1 - \Delta_j(\mathbf{S}, B) + x_j(\mathbf{S}, B))\left(1 + g_j(\mathbf{S}, B)\right) V_{1,k}(\mathbf{S}, B)\right] \end{aligned} \tag{47}$$

until $||V_{1,k+1}(\mathbf{S}, B) - V_{1,k}(\mathbf{S}, B)|| <$ tol. $V_{1,j+1}(\mathbf{S}, B)$ is the converged value function.

6. Update the guess for innovation intensity of incumbents:

$$x_{j+1}(\mathbf{S}, B) = \max\left\{\left[\frac{\theta}{\alpha} \xi^{\frac{1}{\theta}} \frac{\mathbb{E}\left[m_{j+1}(\mathbf{S}, B)\left(1 + g_j(\mathbf{S}, B)\right) V_{1,j+1}(\mathbf{S}, B)\right] - (1 - \alpha) F}{w(\mathbf{S})}\right]^{\frac{\theta}{1-\theta}}, 0\right\}. \tag{48}$$

7. Check for convergence. If $||B'_{j+1}(\mathbf{S}, B) - B'_j(\mathbf{S}, B)|| < \epsilon$ and $||x_{j+1}(\mathbf{S}, B) - x_j(\mathbf{S}, B)|| < \epsilon$ then the problem is solved. Otherwise, discard $B'_j(\mathbf{S}, B)$ and $x'_j(\mathbf{S}, B)$, and use $B'_{j+1}(\mathbf{S}, B)$ and $x'_{j+1}(\mathbf{S}, B)$ as new guesses for the problem (go back to step 1).

Appendix G Persistent Effects of Sudden Stops

We conduct an event analysis around Sudden Stops endogenously generated by the model under the baseline calibration. Using a time window of 10 quarters before and after each event, we average relevant time series.[39] Figure 16 illustrates the Sudden Stop dynamics for the baseline scenario.

Our focus is on the dynamics of five key variables: the value of a product line, the Lagrange multiplier, the current account-to-GDP ratio, the endogenous trend, and log GDP (in levels). Panel (a) shows the evolution of the model's three shocks around the event. In our framework, Sudden Stops typically occur under three conditions: (1) borrowing costs are below their long-run average, (2) interest rate volatility is low and below its long-run average, and (3) a sudden, significant drop in aggregate efficiency takes place. Low and stable borrowing costs promote excessive borrowing, as households do not fully internalize the consequences of their borrowing decisions, leading to overborrowing.[40] These episodes are particularly pronounced when borrowing conditions are favorable. Because efficiency shocks are persistent, the combination of high leverage and a protracted decline in productivity triggers sharp adjustments in borrowing, as depicted in panel (b), where a steep current account reversal follows.

[39] We define a Sudden Stop as an episode where the current account-to-GDP ratio exceeds its long-run average by two standard deviations and the borrowing constraint binds.

[40] This behavior is characteristic of models with occasionally binding borrowing constraints and endogenous collateral values. See Bianchi (2011) and Bianchi and Mendoza (2018) for a detailed analysis of pecuniary externalities in endowment and production models.

Figure 16: Sudden Stop Dynamics - Emerging Economy

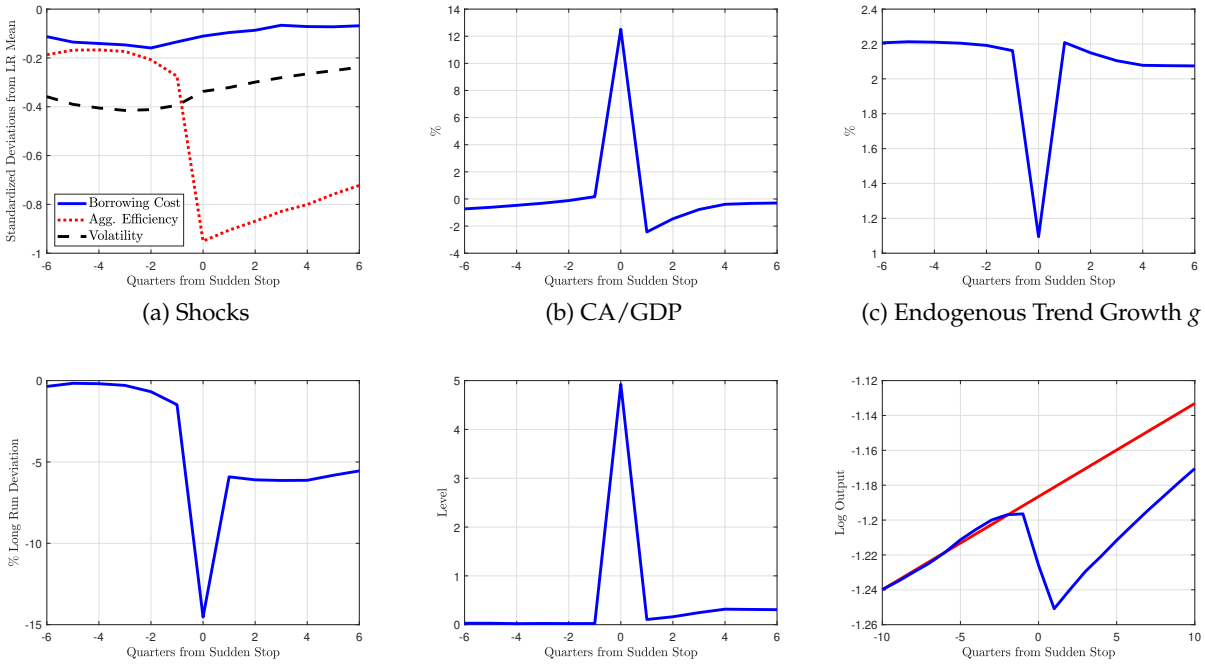

(a) Shocks (b) CA/GDP (c) Endogenous Trend Growth g

(d) Value of a Product Line V_1 (e) Lagrange multiplier μ (f) Log GDP

Notes: Sudden Stops are defined as events where the borrowing constraint binds and where the current account-to-GDP ratio is two standard deviations above its long-run mean. The three shocks of the model are standardized by their corresponding long-run means and standard deviations. CA/GDP denotes the current account-to-GDP ratio, and log GDP corresponds to the log of GDP in levels. The red solid line in the log GDP panel denotes the average trend, which is constructed by averaging the linear growth using the trend growth rate 10 quarters before a Sudden Stop.

Panel (c) depicts the trend growth response: a decline of approximately 1 percentage point (annualized), followed by a rapid recovery. However, as shown in panel (d), the value of a product line experiences a sharp drop and fails to return to its pre-Sudden Stop level. This persistent decline is driven by both the sustained low aggregate efficiency and the increased likelihood of a binding borrowing constraint post-event (panel (e)). A depressed product line value also implies that collateral values remain below their long-run average, contributing to the sluggish recovery. Finally, panel (f) clearly demonstrates the long-lasting consequences, or hysteresis, of a Sudden Stop: output suffers an abrupt and permanent deviation from its pre-event trend.

It is important to distinguish between the crises driven by U.S. interest rate volatility and the Sudden Stops analyzed in this appendix. In the main text, we focus on how increased volatility in U.S. interest rates negatively impacts growth, as agents anticipate larger future interest rate

shocks. This is because adverse rate shocks tend to be more damaging than rate reductions are beneficial for growth in emerging economies. However, as shown here, Sudden Stops are different. These events involve a sharp current account reversal and are typically triggered by large negative TFP shocks. Not every instance of a binding borrowing constraint leads to a Sudden Stop by this definition; the constraint can bind without causing such a large current account reversal. Sudden Stops are more closely linked to deep contractions in aggregate efficiency and borrowing needs for consumption smoothing, whereas the main text centers on the dynamics of interest rate volatility and its asymmetric effects on growth due to a binding constraint, without requiring a sharp current account reversal.

Appendix H Additional Results: Binding Borrowing Constraints

Figure 17 displays simulations of the Lagrange multiplier and the probability of a binding borrowing constraint across three scenarios: baseline, advanced economy calibrations, and an intermediate case with a relaxed borrowing constraint. These simulations incorporate actual interest rate and interest rate volatility data and follow the methodology outlined in Section 4.5. To facilitate comparison, Lagrange multipliers are normalized by their respective ergodic means.

As detailed in Section 4.5, our emerging economy calibration highlights strong precautionary motives among households, as the probability of a binding borrowing constraint remains below 10% during periods of low risk. However, in times of heightened interest rate uncertainty, this probability rises significantly, accompanied by a substantial increase in the effective multiplier. In the other two scenarios, economies generally operate near the borrowing limit, with episodes of increased volatility prompting deleveraging, thereby moving away from the endogenous borrowing limit. The behavior of advanced economies is consistent with the relatively painless amplification triggered by a shock that forces deleverage.

Figure 17: Borrowing Constraint Multiplier & Binding Probability Based on Actual Interest Rate and Volatility Time Series

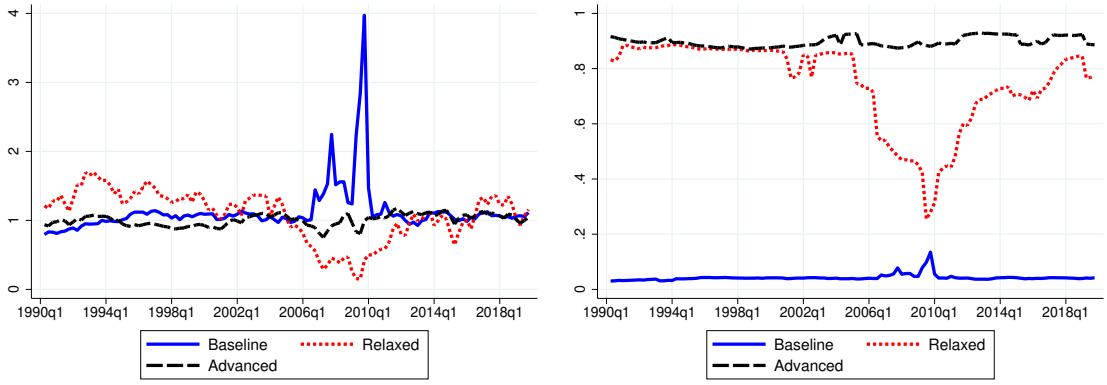

(a) Average Multiplier $\tilde{\mu}$

(b) Prob. of Binding Constraint $\Pr(\tilde{\mu}_t > 0)$

Notes: This figure shows, for the three calibrations (baseline, relaxed constraint, and advanced), the average normalized Lagrange multiplier and the probability of observing a binding borrowing constraint when all economies are subjected to the same path of U.S. real interest rates and volatility. Averages are taken across 10,000 simulated TFP paths.